Lithos 112 (2009) 57–72

Contents lists available at ScienceDirect

Lithos

journal homepage: www.elsevier.com/locate/lithos

# Shallow origin for South Atlantic Dupal Anomaly from lower continental crust: Geochemical evidence from the Mid-Atlantic Ridge at 26°S

Marcel Regelous [a,b,c,*], Yaoling Niu [d], Wafa Abouchami [b], Pat R. Castillo [e]

[a] Department of Earth Sciences, Royal Holloway University of London, Egham, Surrey TW20 0EX, UK
[b] Max Planck Institut für Chemie, Abteilung Geochemie, Postfach 3060, 55020 Mainz, Germany
[c] Department of Earth Science, The University of Queensland, Brisbane 4072, Australia
[d] Department of Earth Sciences, Durham University, Science Labs, Durham DH1 3LE, UK
[e] Scripps Institution of Oceanography, University of California, San Diego, La Jolla, CA 92093-0212, USA

ARTICLE INFO

*Article history:*
Received 23 June 2008
Accepted 20 October 2008
Available online 30 October 2008

*Keywords:*
Mid-Atlantic Ridge
Dupal Anomaly
Continental crust
Flood basalt
Trace elements

ABSTRACT

We measured trace element concentrations and Pb isotope compositions of fresh volcanic glass samples from the Mid-Atlantic Ridge at 26°S, and from nearby off-axis seamounts. The samples have previously been studied for major elements and Sr–Nd–He isotopes. All samples are depleted MORB, and include some of the most incompatible trace element depleted lavas yet reported from the Atlantic. The seamount lavas are more depleted in highly incompatible elements than the axial lavas, but have high Sr, Pb and Eu concentrations, relative to REE of similar incompatibility. The lavas with the highest Sr/Nd, Pb/Ce and Eu/Eu* have the highest $^{3}He/^{4}He$ (up to 11.0 R/RA) ratios and the lowest incompatible trace element concentrations. They also have the highest $^{87}Sr/^{86}Sr$ (up to 0.7036) and $^{208}Pb/^{204}Pb$ for a given $^{206}Pb/^{204}Pb$ ratio, which are characteristics of lavas from the Dupal Anomaly in the South Atlantic, and of many EM-1 type intraplate lavas generally.

Our data place constraints on the origin of the Dupal Anomaly. The enrichments in Sr, Pb and Eu, together with the low Ca/Al ratios of the seamount lavas indicate that their mantle source consists of material that at one time contained plagioclase, and must therefore have resided at crustal pressures. We argue that the trace element and isotopic compositions of the seamount lavas are best explained by derivation from a mantle source contaminated with lower continental crust, which was introduced into the upper mantle during continental rifting and breakup in the South Atlantic. Our results support previous suggestions that the Dupal Anomaly in the South Atlantic has a relatively recent, shallow origin in lower continental crust and continental lithospheric mantle, rather than in recycled material supplied from the deeper mantle by plumes. Plate reconstructions place the Parana–Etendeka flood basalt province over the central part of the Dupal Anomaly at the time of rifting of South America and Africa at 134 Ma. The flood basalts which have undergone the least crustal-level contamination also have extreme Dupal compositions. We speculate that delamination of dense lower continental crust during continental rifting causes flood basalt magmatism, whilst variably polluting the upper oceanic mantle with continental material.



## 1. Introduction

Geochemical studies of lavas from the southern Mid-Atlantic Ridge (MAR) have shown that there are large variations in the trace element and isotope compositions of lavas erupted along this slow-spreading ridge (Hart, 1984; Humphris et al., 1985; Schilling et al., 1985; Hanan et al., 1986; Graham et al., 1992; Fontignie and Schilling, 1996; Douglass et al., 1999; le Roux et al., 2002; Andres et al., 2002; Escrig et al., 2005). In some regions, spike-like trace element and isotope enrichments are thought to result from sublithospheric channeled flows of enriched mantle from off-ridge 'hotspots' to the MAR axis (Schilling et al., 1985; Humphris et al., 1985; Hanan et al., 1986; Fontignie and Schilling, 1996). Longer-wavelength isotopic variations along the length of the southern MAR have been attributed to the dispersal of material from the Tristan da Cunha and Saint Helena 'plume heads', prior to opening of the South Atlantic at about 130 Ma (Hanan et al., 1986; Fontignie and Schilling, 1996; Douglass and Schilling, 2000). Other geochemical variations along the southern MAR appear to be unrelated to sites of active intraplate magmatism, and may instead be derived from passive, lumpy heterogeneities in the upper mantle (Michael et al., 1994).

Many oceanic basalts from the South Atlantic have distinctive isotope compositions, with relatively high $^{87}Sr/^{86}Sr$, and high $^{208}Pb/^{204}Pb$ for a given $^{206}Pb/^{204}Pb$ (Dupré and Allègre, 1983; Hart, 1984;

* Corresponding author. GeoZentrum Nordbayern, Universität Erlangen-Nürnberg, Schlossgarten 5, D-91054 Erlangen, Germany. Tel.: +44 1784 443589; fax: +44 1784 471780.
*E-mail address:* regelous@geol.uni-erlangen-de (M. Regelous).

0024-4937/$ – see front matter © 2008 Elsevier B.V. All rights reserved.
doi:10.1016/j.lithos.2008.10.012

Hawkesworth et al., 1986). Lavas with the isotopic characteristics of the Dupal Anomaly occur on the MAR south of about 24°S, on the intraplate volcanic island of Tristan da Cunha, the aseismic Walvis Ridge and Rio Grande Rise, and the associated Parana–Etendeka flood basalts which were erupted at ~132 Ma at the time of rifting of South America from Africa. The origin of the Dupal Anomaly is debated. The unusual compositions of Dupal lavas may reflect upwelling of recycled material from deeper in the mantle, or they may be the result of contamination of the uppermost mantle beneath the South Atlantic by continental material (Hart, 1984; Hawkesworth et al., 1986; Peate et al., 1999; Escrig et al., 2005; Gibson et al., 2005). In this paper, we report new geochemical data for lavas from the spreading axis and from seamounts close to the Mid-Atlantic Ridge axis at 26°S, an area that is situated far from major active intraplate magmatism. The seamount lavas have Sr–Pb isotope compositions that are typical of the Dupal Anomaly. We argue that the trace element and isotopic characteristics of seamount lavas at this location are best explained by a contribution from lower continental crustal material, which was introduced into the upper mantle during rifting of South America from Africa. We suggest that detachment of lower continental crust into the

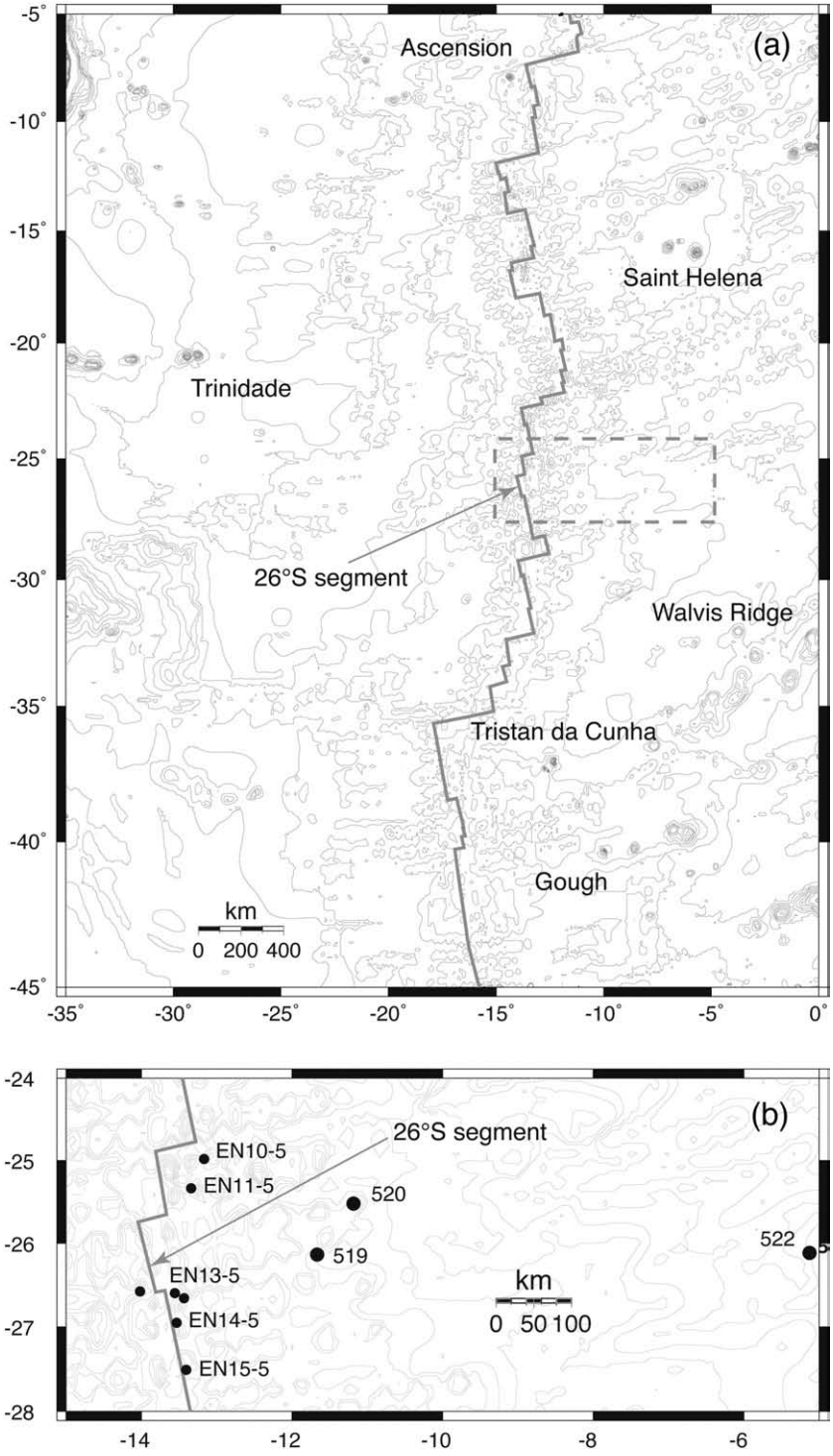


**Fig. 1.** (a) Bathymetric map of the South Atlantic, showing location of the 26°S MAR segment, and sites of intraplate magmatism. (b) Bathymetric map of the Mid-Atlantic Ridge near 26°S, showing locations of the samples analysed from cruise EN063, and DSDP Sites 519, 520 and 522.

upper mantle is an important source of mantle heterogeneity, and speculate that the process of delamination may be responsible for flood basalt magmatism.

## 2. The Mid-Atlantic Ridge at 26°S

The MAR at 26°S is spreading at a rate of ~19.3 mm/yr to the west, and ~16.3 mm/yr to the east (Carbotte et al., 1991). The ridge segment between 25°10′ and 26°35′S is about 100 km long, and is bounded by the Rio Grande Transform to the north, and the Moore Fracture Zone to the south (Fig. 1). This region of the MAR has been the focus of several detailed geological and geophysical studies (Carbotte et al., 1991; Blackman and Forsyth, 1991; Grindlay et al., 1992). There is a topographic high near the centre of the ridge segment, where the axis shallows to about 2600 m depth (Fig. 2). To the north and south of the topographic high, the ridge axis deepens to around 4100 m depth near the transform offsets. Towards the ends of the ridge segment, there is a well-developed axial rift valley, which is up to 25 km wide and 1.5 km deep. The rift valley shallows towards the centre of the segment and is absent at the topographic high.

The samples we have studied have previously been analysed for major elements (Batiza et al., 1988; 1989; Niu and Batiza, 1994), and Sr–Nd–He isotopes (Castillo and Batiza, 1989; Graham et al., 1996). In terms of their major and trace element compositions, all lavas are depleted mid-ocean ridge basalts (N-MORB). Variable low-pressure fractionation of the observed phenocryst phases (olivine, plagioclase and clinopyroxene) can account for the limited range in major element composition of the samples (Niu and Batiza, 1994). Existing isotope data indicate that the mantle underlying this part of the MAR is heterogeneous, and that lavas erupted on the seamounts tend to have more enriched Sr and Nd isotopic compositions than lavas from the ridge axis (Castillo and Batiza, 1989; Graham et al., 1996).

The closest sites of major, active intraplate magmatism in this part of the South Atlantic are at Saint Helena and Trinidade to the north (~1400 and 1600 km from the 26°S segment, respectively), and Tristan da Cunha and Gough Islands to the south (~1300 and 1700 km respectively, Fig. 1a). The 26°S ridge segment is located close to an inferred compositional boundary which separates lavas with Saint Helena-like isotopic characteristics to the north, from lavas with Tristan-Gough-like characteristics to the south (Fontignie and Schilling, 1996).

## 3. Sample locations

Samples prefixed by D- were collected during cruise RC2802 of RV Conrad in 1987 (Batiza et al., 1989). We analysed 22 fresh glass samples from 15 dredge hauls (dredges 12 to 27, average spacing 6–7 km) along the length of the ridge segment (Fig. 2). These samples were collected from within 2 km of the ridge axis, and are therefore younger than about 100 ka.

We also analysed 8 glass samples from 4 dredge hauls (dredges 1, 5, 6 and 7) from seamounts on both the eastern and western flanks of the MAR (see Fig. 2). The ages of these seamounts are uncertain, although the age of the oceanic crust on which they are built places an upper limit on their age. Dredges 5, 6 and 7 are from seamounts

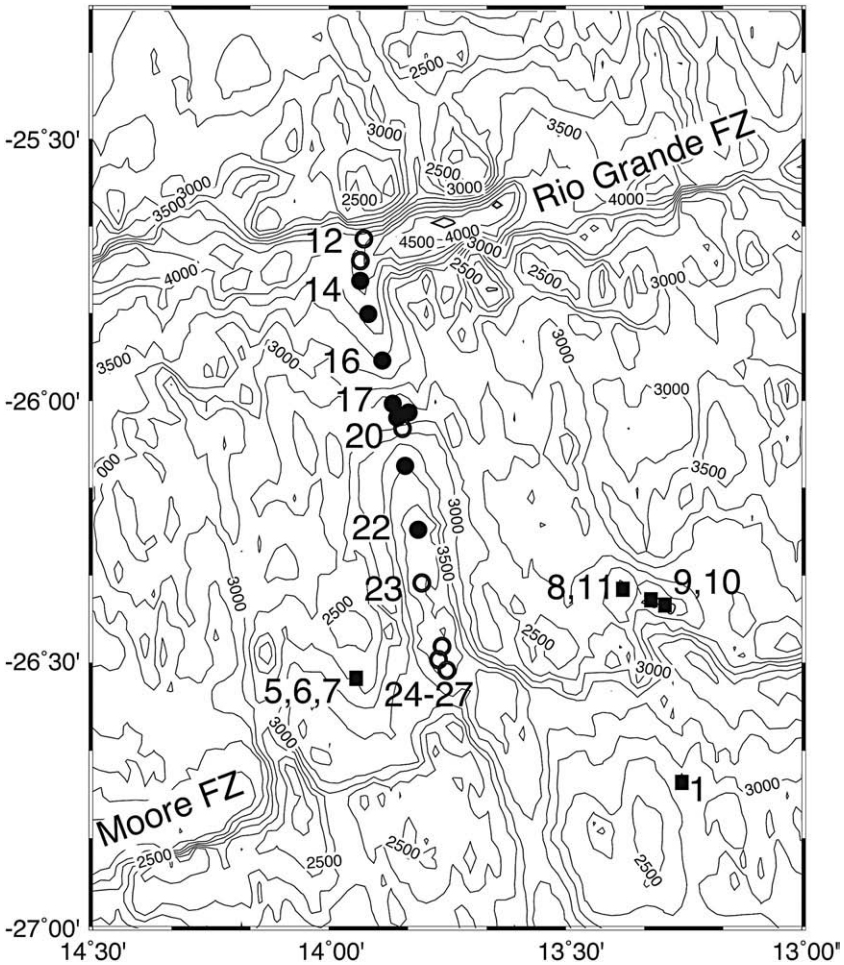


**Fig. 2.** Bathymetric map of the Mid-Atlantic Ridge at 26°S (after Grindlay et al., 1992), showing location of samples recovered during cruise RC2802 (D- prefix in Tables 1 and 2). Dredges which recovered Group 1 and 2 type samples indicated by filled and open circles respectively. Samples from off-ridge seamounts (square symbols) analysed in this study are from dredges 1, 5, 6 and 7.

**Table 1**
Major and trace element data for basaltic glasses from the Mid-Atlantic Ridge at 26°S.

| Sample | D12-23 | D12-29 | D13-7 | D14-1 | D15-2 | D16-2 | D17-3 | D18-3 | D18-5 | D19-1 | D19-2 | D20-1 | D21-1 | D21-5 |
|---|---|---|---|---|---|---|---|---|---|---|---|---|---|---|
| | RA | RA | RA | RA | RA | RA | RA | RA | RA | RA | RA | RA | RA | RA |
| $SiO_2$ | 50.82 | 50.37 | 50.61 | 51.36 | 51.63 | 51.26 | 51.18 | 51.25 | 50.92 | 51.18 | 50.38 | 51.12 | 51.40 | 51.63 |
| $TiO_2$ | 1.65 | 1.60 | 1.58 | 1.57 | 1.51 | 1.38 | 1.37 | 1.34 | 1.30 | 1.18 | 1.23 | 1.38 | 1.53 | 1.27 |
| $Al_2O_3$ | 15.38 | 15.35 | 15.49 | 14.76 | 14.61 | 15.00 | 15.31 | 15.36 | 15.41 | 15.52 | 15.32 | 16.16 | 14.77 | 15.14 |
| FeO | 9.75 | 9.72 | 9.86 | 9.77 | 10.29 | 9.48 | 9.34 | 9.04 | 9.14 | 8.80 | 8.82 | 9.12 | 9.70 | 9.24 |
| MgO | 8.02 | 8.22 | 7.76 | 7.05 | 7.14 | 7.39 | 7.13 | 7.81 | 7.71 | 8.16 | 8.08 | 8.06 | 7.50 | 7.62 |
| CaO | 11.34 | 11.24 | 11.33 | 11.76 | 11.88 | 12.24 | 12.01 | 12.32 | 12.25 | 12.25 | 12.25 | 11.63 | 12.16 | 12.32 |
| $Na_2O$ | 2.72 | 2.72 | 2.58 | 2.94 | 2.76 | 2.64 | 2.83 | 2.78 | 2.82 | 2.63 | 2.56 | 2.70 | 2.63 | 2.79 |
| $K_2O$ | 0.10 | 0.10 | 0.08 | 0.06 | 0.07 | 0.04 | 0.08 | 0.08 | 0.08 | 0.08 | 0.06 | 0.08 | 0.08 | 0.08 |
| $P_2O_5$ | 0.18 | 0.12 | 0.14 | 0.12 | 0.17 | 0.13 | 0.19 | 0.12 | 0.12 | 0.11 | 0.14 | 0.14 | 0.16 | 0.14 |
| Total | 99.96 | 99.44 | 99.54 | 99.36 | 100.06 | 99.56 | 99.44 | 100.10 | 99.75 | 99.91 | 98.84 | 100.39 | 99.93 | 100.23 |
| Li | 6.41 | 6.29 | 6.33 | 5.88 | 6.02 | 5.59 | 5.51 | 5.41 | 5.39 | 5.24 | 5.15 | 5.48 | 4.88 | 5.47 |
| Sc | 35.8 | 35.9 | 35.8 | 38.7 | 39.3 | 38.2 | 38.8 | 39.1 | 37.1 | 37.0 | 36.7 | 34.1 | 32.8 | 38.3 |
| V | 269 | 266 | 261 | 256 | 261 | 249 | 245 | 233 | 234 | 235 | 228 | 230 | 208 | 240 |
| Cr | 326 | 341 | 337 | 231 | 197 | 378 | 344 | 340 | 342 | 385 | 380 | 302 | 397 | 284 |
| Co | 44.5 | 45.4 | 42.5 | 42.1 | 45.6 | 44.6 | 43.4 | 42.1 | 43.3 | 44.5 | 43.3 | 41.6 | 45.1 | 44.2 |
| Ni | 139 | 144 | 118 | 64.6 | 70.9 | 67.8 | 61.2 | 65.6 | 69.2 | 69.8 | 73.0 | 90.9 | 112 | 61.0 |
| Cu | 69.2 | 73.4 | 69.9 | 73.2 | 75.4 | 84.4 | 82.5 | 83.7 | 81.6 | 86.4 | 83.3 | 75.8 | 84.2 | 87.0 |
| Zn | 78.8 | 80.1 | 77.3 | 72.0 | 71.9 | 69.7 | 71.2 | 69.2 | 67.7 | 67.3 | 64.7 | 67.3 | 61.6 | 67.2 |
| Ga | 16.6 | 16.8 | 16.3 | 16.0 | 15.9 | 15.9 | 16.0 | 15.8 | 15.7 | 15.7 | 15.3 | 15.8 | 15.0 | 15.9 |
| Rb | 0.343 | 0.307 | 0.344 | 0.220 | 0.192 | 0.190 | 0.267 | 0.231 | 0.273 | 0.174 | 0.217 | 0.258 | 0.184 | 0.252 |
| Sr | 120 | 120 | 111 | 115 | 104 | 106 | 123 | 120 | 120 | 109 | 108 | 125 | 104 | 114 |
| Y | 31.0 | 30.4 | 31.2 | 27.0 | 27.3 | 24.9 | 25.8 | 25.1 | 24.4 | 23.4 | 23.1 | 25.9 | 20.9 | 24.7 |
| Zr | 105 | 103 | 99.6 | 82.8 | 76.9 | 71.8 | 83.0 | 80.1 | 77.8 | 68.5 | 67.9 | 84.8 | 58.4 | 74.6 |
| Nb | 1.76 | 1.71 | 1.69 | 1.04 | 0.867 | 0.909 | 1.41 | 1.43 | 1.32 | 1.08 | 1.07 | 1.29 | 0.742 | 1.20 |
| Ba | 3.39 | 3.45 | 3.38 | 2.35 | 2.07 | 1.99 | 3.01 | 2.86 | 2.81 | 2.23 | 2.20 | 2.67 | 1.71 | 2.63 |
| La | 3.30 | 3.29 | 3.05 | 2.48 | 2.22 | 2.12 | 2.69 | 2.57 | 2.53 | 2.18 | 2.09 | 2.63 | 1.72 | 2.35 |
| Ce | 11.3 | 11.1 | 10.5 | 8.83 | 7.98 | 7.66 | 9.13 | 8.62 | 8.67 | 7.46 | 7.26 | 9.12 | 6.21 | 8.13 |
| Pr | 2.01 | 1.98 | 1.91 | 1.64 | 1.52 | 1.42 | 1.65 | 1.55 | 1.56 | 1.36 | 1.33 | 1.64 | 1.16 | 1.48 |
| Nd | 10.6 | 10.5 | 10.2 | 8.75 | 8.30 | 7.79 | 8.68 | 8.32 | 8.25 | 7.39 | 7.27 | 8.74 | 6.31 | 7.95 |
| Sm | 3.66 | 3.54 | 3.67 | 3.19 | 3.08 | 2.86 | 3.11 | 2.87 | 2.94 | 2.63 | 2.63 | 3.09 | 2.38 | 2.87 |
| Eu | 1.33 | 1.31 | 1.32 | 1.20 | 1.20 | 1.10 | 1.16 | 1.12 | 1.11 | 1.04 | 1.02 | 1.15 | 0.914 | 1.11 |
| Tb | 0.856 | 0.840 | 0.861 | 0.744 | 0.755 | 0.68 | 0.71 | 0.690 | 0.672 | 0.652 | 0.631 | 0.710 | 0.564 | 0.681 |
| Gd | 4.82 | 4.80 | 4.81 | 4.91 | 4.26 | 3.83 | 4.06 | 3.94 | 3.87 | 3.64 | 3.56 | 4.06 | 3.19 | 3.88 |
| Dy | 5.79 | 5.72 | 5.80 | 5.06 | 5.04 | 4.65 | 4.84 | 4.67 | 4.62 | 4.43 | 4.32 | 4.82 | 3.87 | 4.67 |
| Ho | 1.24 | 1.23 | 1.25 | 1.09 | 1.10 | 0.986 | 1.03 | 1.01 | 0.982 | 0.95 | 0.916 | 1.02 | 0.830 | 0.984 |
| Er | 3.52 | 3.46 | 3.55 | 3.09 | 3.10 | 2.81 | 2.93 | 2.85 | 2.79 | 2.67 | 2.62 | 2.92 | 2.37 | 2.80 |
| Tm | 0.525 | 0.516 | 0.53 | 0.462 | 0.462 | 0.416 | 0.439 | 0.424 | 0.413 | 0.398 | 0.393 | 0.432 | 0.353 | 0.414 |
| Yb | 3.32 | 3.27 | 3.39 | 2.90 | 2.93 | 2.65 | 2.77 | 2.70 | 2.63 | 2.52 | 2.51 | 2.78 | 2.27 | 2.68 |
| Lu | 0.509 | 0.494 | 0.509 | 0.440 | 0.439 | 0.400 | 0.416 | 0.411 | 0.393 | 0.380 | 0.374 | 0.419 | 0.337 | 0.399 |
| Hf | 2.86 | 2.81 | 2.82 | 2.33 | 2.20 | 2.05 | 2.29 | 2.27 | 2.13 | 1.98 | 1.95 | 2.34 | 1.67 | 2.10 |
| Pb | 0.437 | 0.450 | 0.415 | 0.358 | 0.337 | 0.314 | 0.395 | 0.377 | 0.365 | 0.317 | 0.302 | 0.370 | 0.255 | 0.328 |
| Th | 0.100 | 0.097 | 0.095 | 0.061 | 0.052 | 0.052 | 0.077 | 0.076 | 0.074 | 0.061 | 0.059 | 0.073 | 0.042 | 0.067 |
| U | 0.049 | 0.047 | 0.045 | 0.029 | 0.026 | 0.026 | 0.043 | 0.039 | 0.039 | 0.30 | 0.030 | 0.036 | 0.021 | 0.032 |

Major element concentrations in wt.% by electron probe analysis of basaltic glass (Niu and Batiza, 1994). Trace element concentrations (in ppm) determined by ICP-MS on fresh, handpicked glasses, which were leached in a 1:1 mixture of 2 M HCl–$H_2O_2$ for 10 min before dissolution. Analyses were carried out using a Fisons Plasmaquad II ICP-MS instrument at the University of Queensland; reproducibility for most of the elements listed is in the range 1–5%. A detailed description of sample preparation techniques and analytical conditions is given in Niu and Batiza (1997). RA: samples from ridge axis. SMT: samples from off-axis seamounts.

located on seafloor which is approximately 1.8 Ma old, whereas dredge 1 recovered basalt from a seamount on 2.0 Ma old crust. On the basis of the relatively fresh appearance of the seamount glasses, and the fact that they are generally more primitive than lavas from the rift axis, Batiza et al. (1989) speculated that most of the seamounts were formed outside the axial rift valley.

For comparison, we also measured Sr and Pb isotope compositions of 5 glass samples dredged during the Endeavor EN063 cruise from the ridge segments immediately to the south and north of the 26°S segment. Sample locations and other data for these samples are given in Hanan et al. (1986) and Fontignie and Schilling (1996). In addition, we measured Sr and Pb isotope compositions of 5 samples of glass recovered by drilling from older seafloor to the east of the ridge axis at DSDP Sites 519, 520 and 522 (Fig. 1b), which are located on seafloor that is approximately 10.1, 14.3 and 38.4 Ma respectively.

## 4. Analytical methods

All trace element and isotope measurements were carried out on fresh glass chips, which were handpicked in order to avoid fragments which showed signs of alteration, or which contained olivine and plagioclase phenocrysts. Before digestion for trace element and isotope analysis, samples were leached for 10 min at room temperature (2 min in ultrasound) in a 1:1 mixture of $H_2O_2$ and 2.0 M HCl, and rinsed with Milli-Q water.

Trace element analyses (Table 1) were carried out on a Fisons Plasmaquad II inductively-coupled plasma mass spectrometer at The University of Queensland. Reproducibility for the elements in Table 1 is in the range 1–5%, except for Co and Th (~7%). A detailed description of sample preparation techniques and analytical conditions is given by Niu and Batiza (1997).

Most of the Sr and Nd isotope analyses were carried out using a VG54-30 Sector mass spectrometer at the University of Queensland (see Regelous et al., 1999 for analytical details). During the period of analysis, the NBS-987 Sr standard yielded $^{87}Sr/^{86}Sr = 0.710267 \pm 15$ ($2\sigma, n = 10$), and an Ames Nd standard gave $^{143}Nd/^{144}Nd = 0.511969 \pm 9$ ($2\sigma, n = 5$). Data in Table 2 have been normalised to values of 0.710265 and 0.511977 (the value of the Ames Nd standard relative to a value of 0.511860 for the La Jolla standard), so that our data can be compared directly with those of Castillo and Batiza (1989). The DSDP Leg 73 samples and the 5

| D22-6 | D22-10 | D23-4 | D23-8 | D24-1 | D25-1 | D27-1 | D27-3 | D1-1 | D5-5 | D6-3 | D6-4 | D7-4 | D7-5 |
|---|---|---|---|---|---|---|---|---|---|---|---|---|---|
| RA | RA | RA | RA | RA | RA | RA | RA | SMT | SMT | SMT | SMT | SMT | SMT |
| 51.75 | 51.42 | 50.63 | 50.59 | 50.86 | 50.06 | 50.94 | 50.76 | 50.89 | 49.80 | 49.26 | 48.72 | 49.39 | 49.56 |
| 1.26 | 1.73 | 1.70 | 1.68 | 1.54 | 1.41 | 1.41 | 1.38 | 1.58 | 1.12 | 1.27 | 1.25 | 1.16 | 1.19 |
| 14.97 | 14.26 | 15.26 | 15.26 | 15.49 | 15.74 | 15.85 | 15.49 | 15.65 | 17.59 | 17.59 | 17.49 | 17.32 | 17.41 |
| 9.21 | 11.02 | 9.91 | 9.88 | 9.54 | 9.48 | 9.14 | 9.39 | 9.22 | 9.21 | 8.75 | 9.10 | 8.82 | 9.13 |
| 8.52 | 6.55 | 7.54 | 7.53 | 8.00 | 8.08 | 8.08 | 8.23 | 7.76 | 8.48 | 8.44 | 8.81 | 8.28 | 8.41 |
| 12.44 | 11.16 | 11.46 | 11.48 | 11.51 | 11.68 | 11.79 | 11.72 | 11.41 | 11.19 | 11.49 | 11.34 | 11.37 | 11.18 |
| 2.58 | 2.96 | 2.71 | 2.69 | 2.81 | 2.70 | 2.40 | 2.43 | 2.79 | 2.87 | 3.00 | 3.06 | 2.84 | 2.87 |
| 0.07 | 0.07 | 0.09 | 0.08 | 0.07 | 0.06 | 0.07 | 0.07 | 0.10 | 0.05 | 0.06 | 0.07 | 0.06 | 0.05 |
| 0.11 | 0.15 | 0.16 | 0.15 | 0.16 | 0.17 | 0.12 | 0.11 | 0.17 | 0.12 | 0.11 | 0.14 | 0.10 | 0.09 |
| 99.91 | 99.32 | 99.46 | 99.34 | 99.98 | 99.38 | 99.80 | 99.58 | 99.57 | 100.43 | 99.97 | 99.98 | 99.34 | 99.89 |
| 4.86 | 6.08 | 6.64 | 6.47 | 6.05 | 5.67 | 5.87 | 5.84 | 6.11 | 4.69 | 4.83 | 4.83 | 4.60 | 4.47 |
| 35.3 | 39.1 | 37.6 | 36.3 | 34.8 | 33.2 | 34.2 | 35.7 | 33.7 | 31.9 | 32.9 | 32.3 | 32.0 | 31.7 |
| 215 | 263 | 282 | 279 | 259 | 239 | 245 | 248 | 254 | 168 | 175 | 174 | 174 | 178 |
| 390 | 255 | 292 | 290 | 350 | 331 | 387 | 370 | 338 | 297 | 415 | 415 | 385 | 328 |
| 43.2 | 43.9 | 42.4 | 43.4 | 43.7 | 44.0 | 45.0 | 43.3 | 45.2 | 47.5 | 49.4 | 49.1 | 48.7 | 48.9 |
| 80.6 | 68.4 | 90.1 | 94.4 | 114 | 142 | 181 | 152 | 144 | 173 | 223 | 223 | 212 | 199 |
| 80.6 | 68.3 | 69.8 | 73.3 | 71.5 | 70.1 | 65.8 | 72.1 | 72.4 | 116 | 91.4 | 89.7 | 107 | 111 |
| 60.3 | 74.3 | 79.8 | 82.5 | 75.6 | 70.0 | 70.2 | 75.2 | 76.8 | 64.8 | 62.5 | 60.5 | 64.4 | 64.4 |
| 15.0 | 16.4 | 16.9 | 17.2 | 16.6 | 15.8 | 15.2 | 16.1 | 16.6 | 16.2 | 15.1 | 15.1 | 15.9 | 15.8 |
| 0.184 | 0.261 | 0.354 | 0.314 | 0.274 | 0.267 | 0.285 | 0.253 | 0.370 | 0.095 | 0.101 | 0.145 | 0.122 | 0.128 |
| 108 | 111 | 114 | 113 | 116 | 116 | 104 | 107 | 129 | 190 | 193 | 190 | 173 | 173 |
| 21.0 | 27.7 | 33.7 | 32.0 | 28.8 | 26.8 | 27.1 | 28.1 | 29.0 | 19.0 | 21.4 | 21.2 | 20.1 | 20.3 |
| 59.3 | 83.1 | 109 | 104 | 93.8 | 88.2 | 87.8 | 89.9 | 103 | 64.9 | 83.5 | 82.1 | 66.6 | 67.4 |
| 0.930 | 1.06 | 1.70 | 1.66 | 1.25 | 1.29 | 1.35 | 1.37 | 1.97 | 0.694 | 0.833 | 0.895 | 0.836 | 0.833 |
| 2.26 | 2.48 | 3.49 | 3.39 | 2.63 | 2.52 | 2.67 | 2.79 | 4.20 | 1.12 | 1.26 | 1.36 | 1.45 | 1.43 |
| 1.86 | 2.46 | 3.26 | 3.20 | 2.82 | 2.73 | 2.71 | 2.80 | 3.52 | 2.24 | 2.86 | 2.84 | 2.24 | 2.25 |
| 6.50 | 8.85 | 11.3 | 11.1 | 10.0 | 9.44 | 9.27 | 9.48 | 11.8 | 7.38 | 9.41 | 9.37 | 7.43 | 7.46 |
| 1.20 | 1.62 | 2.07 | 2.02 | 1.85 | 1.70 | 1.67 | 1.71 | 2.07 | 1.30 | 1.62 | 1.60 | 1.30 | 1.30 |
| 6.51 | 8.80 | 11.1 | 10.8 | 9.81 | 9.07 | 8.78 | 9.11 | 10.7 | 6.72 | 8.16 | 8.14 | 6.87 | 6.84 |
| 2.35 | 3.27 | 4.01 | 3.75 | 3.45 | 3.15 | 3.12 | 3.14 | 3.55 | 2.27 | 2.61 | 2.64 | 2.36 | 2.32 |
| 0.946 | 1.22 | 1.40 | 1.35 | 1.28 | 1.17 | 1.13 | 1.17 | 1.31 | 0.948 | 1.05 | 1.06 | 0.985 | 0.983 |
| 0.583 | 0.771 | 0.932 | 0.893 | 0.814 | 0.744 | 0.751 | 0.768 | 0.820 | 0.529 | 0.595 | 0.596 | 0.557 | 0.560 |
| 3.26 | 4.33 | 5.21 | 5.04 | 4.58 | 4.22 | 4.21 | 4.34 | 4.67 | 3.07 | 3.44 | 3.42 | 3.18 | 3.22 |
| 3.94 | 5.18 | 6.29 | 6.02 | 5.42 | 5.03 | 5.03 | 5.22 | 5.46 | 3.57 | 4.00 | 4.00 | 3.80 | 3.80 |
| 0.857 | 1.10 | 1.33 | 1.29 | 1.14 | 1.07 | 1.08 | 1.13 | 1.17 | 0.764 | 0.861 | 0.856 | 0.820 | 0.816 |
| 2.40 | 3.12 | 3.80 | 3.64 | 3.28 | 3.06 | 3.10 | 3.20 | 3.30 | 2.16 | 2.42 | 2.41 | 2.30 | 2.30 |
| 0.362 | 0.462 | 0.567 | 0.544 | 0.492 | 0.450 | 0.464 | 0.486 | 0.491 | 0.320 | 0.365 | 0.364 | 0.345 | 0.348 |
| 2.28 | 2.99 | 3.66 | 3.44 | 3.13 | 2.91 | 2.98 | 3.07 | 3.12 | 2.04 | 2.31 | 2.31 | 2.19 | 2.21 |
| 0.342 | 0.444 | 0.549 | 0.522 | 0.465 | 0.437 | .454 | 0.469 | 0.468 | 0.312 | 0.352 | 0.352 | 0.338 | 0.339 |
| 1.73 | 2.34 | 2.99 | 2.90 | 2.62 | 2.45 | 2.45 | 2.51 | 2.77 | 1.74 | 2.09 | 2.05 | 1.80 | 1.78 |
| 0.295 | 0.352 | 0.432 | 0.429 | 0.390 | 0.374 | 0.365 | 0.278 | 0.468 | 0.393 | 0.484 | 0.503 | 0.386 | 0.384 |
| 0.052 | 0.062 | 0.098 | 0.094 | 0.070 | 0.072 | 0.076 | 0.080 | 0.110 | 0.049 | 0.056 | 0.058 | 0.053 | 0.054 |
| 0.026 | 0.029 | 0.045 | 0.046 | 0.034 | 0.036 | 0.037 | 0.039 | 0.053 | 0.020 | 0.025 | 0.026 | 0.022 | 0.022 |

samples provided by J.-G. Schilling were analysed for Sr isotopes at the Max-Planck Institut für Chemie, using a Finnigan Triton mass spectrometer, and normalised to the same values for the NBS-987 standard as the other analyses.

Pb isotope analyses were carried out at the Max-Planck Institut für Chemie, using a triple-spike technique (Galer, 1999) to correct for instrumental mass fractionation (see Regelous et al., 2002 for details). Most of the analyses were carried out on a Finnigan 261 instrument, which yielded values of $^{206}Pb/^{204}Pb = 16.9403 \pm 22$, $^{207}Pb/^{204}Pb = 15.4974 \pm 20$, and $^{208}Pb/^{204}Pb = 36.7246 \pm 58$ ($2\sigma$, $n = 22$) for the NBS-981 Pb standard. The DSDP Leg 73 samples, and the samples prefixed by EN- were analysed at a later time by triple spiking using a Finnigan Triton mass spectrometer; these data have been normalised to the same values for the NBS981 standard as the earlier analyses.

## 5. Results

New trace element data for lavas from the ridge axis and from near ridge seamounts at 26°S are given in Table 1, and Sr, Nd and Pb isotope data in Table 2. Sr and Pb isotope data for glasses from adjacent ridge segments, and from older crust drilled on DSDP Leg 73 are listed in Table 3. In the following figures, we show the new triple-spike Pb isotope data rather than the conventional data presented in Castillo and Batiza (1989) and Graham et al. (1996). Following Niu and Batiza (1994), we have divided the samples from the ridge axis into two groups, according to whether plagioclase (Group 1) or olivine (Group 2) was apparently the first liquidus phase.

### 5.1. Lavas from the ridge axis

The variations in trace element composition of lavas from the ridge axis are small, compared to many other individual ridge segments elsewhere on the MAR which have been studied in detail (Niu et al., 2001; Michael et al., 1994). All samples are 'normal' depleted MORB ($La/Sm_N$ 0.50–0.65), and have low concentrations of the highly incompatible elements such as Rb, Ba, Th and low ratios of highly- to moderately-incompatible elements, compared to most other Atlantic MORB (Fig. 3). Lavas with the highest incompatible trace element concentrations and highest La/Sm ratios tend to occur on the

**Table 2**
Sample locations and Sr, Nd and Pb isotope data for basaltic glasses from the Mid-Atlantic Ridge axis at 26°S.

| Sample | | Latitude (°S) | Longitude (°W) | Depth (m) | $^{87}Sr/^{86}Sr$ | $^{143}Nd/^{144}Nd$ | $^{206}Pb/^{204}Pb$ | $^{207}Pb/^{204}Pb$ | $^{208}Pb/^{204}Pb$ |
|---|---|---|---|---|---|---|---|---|---|
| D12-23 | RA | 25.70 | 13.92 | 3980 | 0.702554 | 0.513107 | 18.2894 ± 13 | 15.5034 ± 15 | 37.9158 ± 44 |
| D12-29 | RA | 25.70 | 13.92 | 3980 | *0.702552* | *0.513086* | | | |
| D13-7 | RA | 25.73 | 13.93 | 3920 | 0.702529 | 0.513106 | 18.2469 ± 10 | 15.4947 ± 11 | 37.8509 ± 32 |
| D14-1 | RA | 25.77 | 13.94 | 3985 | 0.702516 | 0.513105 | 18.2001 ± 9 | 15.4880 ± 11 | 37.7970 ± 31 |
| D15-2 | RA | 25.84 | 13.91 | 3920 | 0.702469 | 0.513119 | 18.1241 ± 12 | 15.4824 ± 12 | 37.7209 ± 35 |
| D16-2 | RA | 25.93 | 13.87 | 3465 | 0.702527 | 0.513124 | | | |
| D17-3 | RA | 26.00 | 13.88 | 2675 | 0.702588 | | | | |
| D18-3 | RA | 26.02 | 13.88 | 2510 | *0.702525* | *0.513120* | | | |
| D18-5 | RA | 26.02 | 13.88 | 2510 | 0.702605 | 0.513084 | 18.3720 ± 10 | 15.5140 ± 12 | 38.0042 ± 38 |
| D19-1 | RA | 26.01 | 13.84 | 2530 | *0.702550* | *0.513076* | 18.3605 ± 12 | 15.5117 ± 12 | 37.9922 ± 38 |
| D19-2 | RA | 26.01 | 13.84 | 2530 | 0.702549 | 0.513077 | 18.3584 ± 11 | 15.5092 ± 11 | 37.9841 ± 33 |
| D20-1 | RA | 26.04 | 13.87 | 2705 | 0.702535 | 0.513100 | 18.2761 ± 13 | 15.4987 ± 13 | 37.8909 ± 36 |
| D21-1 | RA | 26.12 | 13.86 | 3380 | 0.702521 | 0.513143 | 18.1347 ± 11 | 15.4865 ± 13 | 37.7377 ± 40 |
| D21-5 | RA | 26.12 | 13.86 | 3380 | 0.702539 | 0.513115 | 18.2394 ± 8 | 15.4958 ± 9 | 37.8435 ± 28 |
| D22-6 | RA | 26.23 | 13.82 | 3785 | *0.702521* | *0.513138* | | | |
| D22-10 | RA | 26.23 | 13.82 | 3785 | 0.702496 | 0.513113 | 18.1968 ± 10 | 15.4896 ± 11 | 37.7952 ± 32 |
| D23-4 | RA | 26.33 | 13.79 | 3705 | 0.702582 | 0.513109 | 18.3079 ± 12 | 15.5014 ± 11 | 37.9257 ± 32 |
| D23-8 | RA | 26.33 | 13.79 | 3705 | *0.702577* | *0.513118* | | | |
| D24-1 | RA | 26.44 | 13.76 | 3480 | 0.702518 | 0.513131 | 18.2153 ± 10 | 15.4955 ± 11 | 37.8304 ± 33 |
| D25-1 | RA | 26.47 | 13.77 | 3760 | 0.702531 | 0.513107 | | | |
| D27-1 | RA | 26.49 | 13.75 | 3700 | 0.702541 | 0.513106 | 18.2452 ± 11 | 15.4953 ± 11 | 37.8583 ± 32 |
| D27-3 | RA | 26.49 | 13.75 | 3700 | *0.702538* | *0.513106* | 18.2489 ± 12 | 15.4989 ± 13 | 37.8694 ± 39 |
| D1-1 | SMT | 26.73 | 13.22 | 2800 | *0.702595* | *0.513093* | 18.3144 ± 10 | 15.5049 ± 10 | 37.9569 ± 30 |
| D5-5 | SMT | 26.54 | 13.91 | 2500 | *0.703629* | *0.512919* | | | |
| D5-7 | SMT | 26.54 | 13.91 | 2500 | 0.703560 | | 18.2274 ± 11 | 15.5409 ± 11 | 38.1540 ± 34 |
| D5-8 | SMT | 26.54 | 13.91 | 2500 | 0.703559 | | 18.2411 ± 22 | 15.5476 ± 21 | 38.1807 ± 57 |
| D6-3 | SMT | 26.58 | 13.91 | 2930 | *0.703098* | *0.512973* | 18.3376 ± 10 | 15.5301 ± 10 | 38.1610 ± 28 |
| D6-4 | SMT | 26.58 | 13.91 | 2930 | *0.703155* | *0.512954* | 18.3276 ± 11 | 15.5292 ± 12 | 38.1644 ± 38 |
| D7-4 | SMT | 26.55 | 13.92 | 2375 | *0.703430* | *0.512988* | 18.3059 ± 10 | 15.5407 ± 11 | 38.1744 ± 33 |
| D7-4 (A) | SMT | 26.55 | 13.92 | 2375 | | | 18.6497 ± 9 | 15.6227 ± 9 | 38.5933 ± 28 |
| D7-5 | SMT | 26.55 | 13.92 | 2375 | *0.703475* | *0.512985* | 18.3049 ± 13 | 15.5394 ± 16 | 38.1720 ± 51 |

Data in italics are from Castillo and Batiza (1989), Graham et al. (1996); other Sr and Nd isotope analyses carried out at the University of Queensland on fresh, handpicked glasses which were leached for 10 min in a 1:1 mixture of 2 M HCl and $H_2O_2$, and rinsed thoroughly with MQ $H_2O$ before dissolution. Sr and Nd isotope analyses were carried out on a VG54 sector instrument, and corrected for mass fractionation using $^{86}Sr/^{88}Sr = 0.1194$ and $^{146}Nd/^{144}Nd = 0.7219$. All data normalised to values of 0.710265 and 0.511860 for the NBS-987 Sr and La Jolla Nd standards. Pb isotope analyses carried out at the MPI Mainz, using a triple spike method to correct for instrumental mass fractionation, which yielded values for the NBS-981 standard of 16.9403 ± 22, 15.4974 ± 20, 36.7246 ± 58 for $^{206}Pb/^{204}Pb$, $^{207}Pb/^{204}Pb$ and $^{208}Pb/^{204}Pb$ respectively. D7-4 (A) is an analysis of Fe–Mn material coating glass from sample D7-4. RA and SMT indicate samples from ridge axis and from off-axis seamounts respectively.

axial high close to the segment centre, and at the segment ends (Batiza et al., 1989).

Sr and Nd isotope compositions of lavas from the ridge axis at 26°S show little variation (Fig. 4b), and lie within the range of previously reported data from the Mid-Atlantic Ridge between 3 and 46°S (Hanan et al., 1986; Fontignie and Schilling, 1996). Samples with the highest $^{87}Sr/^{86}Sr$ and lowest $^{143}Nd/^{144}Nd$ ratios occur at the ends and at the centre of the ridge segment. Pb isotope ratios also lie within the range of previously reported data from the South Atlantic. However, the more precise triple-spike Pb isotope data define remarkable linear arrays in the $^{207}Pb/^{204}Pb$- and $^{208}Pb/^{204}Pb$–$^{206}Pb/^{204}Pb$ diagrams (Fig. 5). $^{206}Pb/^{204}Pb$ correlates positively with $^{87}Sr/^{86}Sr$, and negatively with $^{143}Nd/^{144}Nd$. The new data confirm the positive correlation between $^{206}Pb/^{204}Pb$ and $^{4}He/^{3}He$ reported by Graham et al. (1996). $^{206}Pb/^{204}Pb$ ratios also correlate with incompatible trace element ratios such as La/Sm, Nb/Zr, and with the concentrations of incompatible elements.

**Table 3**
Sr and Pb isotope data for other South Atlantic MORB glass samples.

| Sample | Age (Ma) | $^{87}Sr/^{86}Sr$ measured | $^{87}Sr/^{86}Sr$ initial | $^{206}Pb/^{204}Pb$ measured | $^{207}Pb/^{204}Pb$ measured | $^{208}Pb/^{204}Pb$ measured | $^{206}Pb/^{204}Pb$ age corrected | $^{207}Pb/^{204}Pb$ age corrected | $^{208}Pb/^{204}Pb$ age corrected |
|---|---|---|---|---|---|---|---|---|---|
| EN063 10D-5g | 0 | 0.702553 | | 18.3323 ± 34 | 15.5030 ± 37 | 37.9456 ± 115 | | | |
| EN063 10D-5g rpt | 0 | | | 18.3315 ± 28 | 15.5028 ± 37 | 37.9453 ± 119 | | | |
| EN063 11D-5g | 0 | 0.702615 | | 18.1474 ± 26 | 15.4902 ± 32 | 37.8360 ± 105 | | | |
| EN063 13D-5g | 0 | 0.702567 | | 18.3093 ± 24 | 15.5036 ± 30 | 37.9321 ± 97 | | | |
| EN063 14D-5g | 0 | 0.702541 | | 18.3003 ± 25 | 15.5001 ± 31 | 37.9043 ± 101 | | | |
| EN063 15D-5g | 0 | 0.702622 | | 18.3181 ± 27 | 15.5044 ± 34 | 37.9585 ± 110 | | | |
| 73 519A 8R-4 139–143 | 10.1 | 0.702637 | 0.702636 | 18.5172 ± 28 | 15.5297 ± 34 | 38.1839 ± 112 | 18.5076 | 15.5292 | 38.1775 |
| 73 520 30R-1 69–74 | 14.3 | 0.702644 | 0.702643 | 18.3209 ± 21 | 15.5116 ± 26 | 38.0071 ± 86 | 18.3073 | 15.5110 | 37.9981 |
| 73 520 30R-1 81–86 | 14.3 | | | 18.3492 ± 23 | 15.5091 ± 30 | 38.0273 ± 96 | 18.3356 | 15.5085 | 38.0182 |
| 73 522 3R-4 2–4 | 38.4 | 0.702995 | 0.702991 | 18.1366 ± 21 | 15.5054 ± 26 | 37.9930 ± 83 | 18.1003 | 15.5037 | 37.9688 |
| 73 522 3R-4 2–4 rpt* | 38.4 | 0.702983 | 0.702979 | | | | | | |

Sr and Pb isotope measurements carried out on handpicked, leached glasses at M.P.I. on a Triton multicollector mass spectrometer in static mode, except Sr analysis 73 522 3R-4 2–4 rpt, which was carried out on a separate dissolution of 5 mg handpicked, leached glass at Royal Holloway using a 5-collector VG54 sector mass spectrometer in dynamic mode. All data normalised to values of 0.710265 and 0.511860 for the NBS-987 Sr and La Jolla Nd standards. Pb isotope analyses by triple spike at the M.P.I. Mainz, using a Finnigan Triton mass spectrometer; during the period of analysis the NBS-981 Pb isotope standard yielded $^{206}Pb/^{204}Pb$, $^{207}Pb/^{204}Pb$ and $^{208}Pb/^{204}Pb$ ratios of 16.9447, 15.5024 and 36.7350 respectively, and sample data have been normalised to the same values for NBS-981 as data in Table 2. Sr and Pb isotope data for off-axis samples age-corrected assuming Rb/Sr, U/Pb and Th/Pb ratios of 0.00226, 0.097 and 0.196 respectively (average values for axial samples in Table 1. Nd isotope data for samples with EN- prefix are given in Fontignie and Schilling (1996).

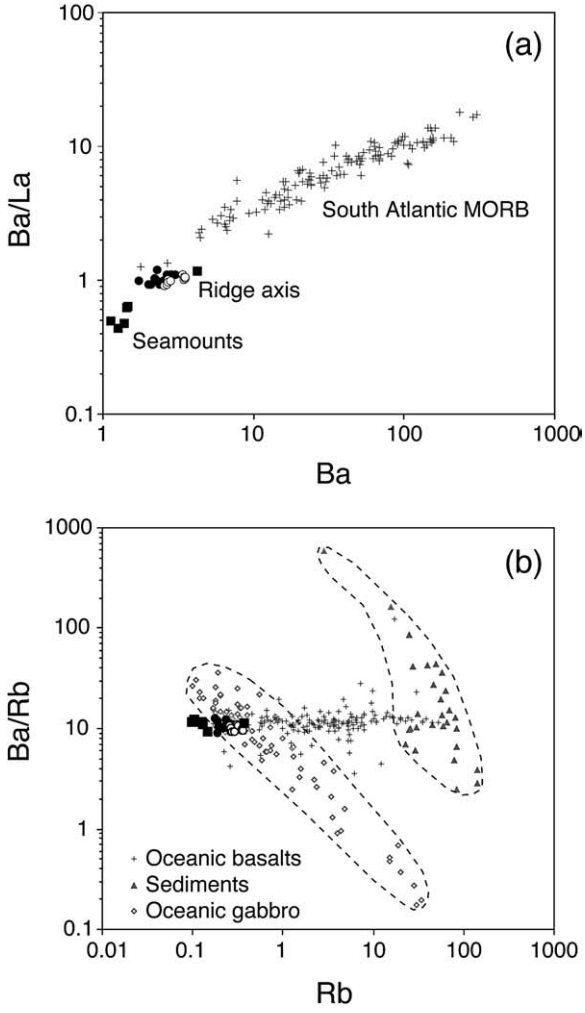


**Fig. 3.** Variation of (a) Ba/La with Ba, and (b) Ba/Rb with Rb, illustrating the low concentrations of highly incompatible trace elements in the seamount lavas compared to other Atlantic MORB, and their uniform Ba/Rb ratios, which are similar to those of other fresh MORB and distinct from those of both oceanic gabbros and sediments. Filled circles: Group 1 glasses from ridge axis; circles: Group 2 glasses from ridge axis; squares: glasses from seamounts. Atlantic MORB data in (a) from Hannigan et al. (2001), le Roex et al. (1990). Global MORB data in (b) from Hofmann and White (1983), Regelous et al. (1999), Niu et al. (1999). Trace element data for oceanic gabbros from Hart et al. (1999) and Coogan et al. (2001). Sediment data are weighted average subducting compositions of Plank and Langmuir (1998).

### 5.2. Seamount lavas

Samples from dredges 1 and 10 have similar compositions to lavas from the ridge axis (Table 1, 2, see also Castillo and Batiza, 1989). Possibly, these lavas were originally erupted at the ridge axis. In contrast, dredges 5, 6 and 7 (from a single large seamount and related cones), recovered glasses with very different major and trace element and isotope compositions to the lavas from the ridge axis.

The seamount lavas from dredges 5, 6, 7 are less evolved, and at a given MgO value they have higher $Al_2O_3$, $Na_2O$, and lower $SiO_2$ than the ridge axis lavas, but similar FeO, CaO and K/Ti. These differences in major element composition may result partly from smaller degrees of melting at higher pressure beneath the seamounts (Batiza et al., 1988), and partly from the different crystallisation histories of the axial and seamount lavas (Batiza et al., 1988; Niu and Batiza, 1994).

Compared to lavas from the ridge axis, the seamount lavas are depleted in highly incompatible elements. Rb and Ba concentrations of these samples are the lowest yet reported for Atlantic MORB and extend to lower values than the highly depleted lavas from the Garrett Transform in the Pacific (Wendt et al., 1999). Compared to lavas from the adjacent ridge axis (and to average N-MORB), the seamount lavas have high Sr, Pb and Eu relative to REE of similar incompatibility (Fig. 6). Pb/Ce ratios (0.052–0.054) are higher than those typical of oceanic basalts (0.033–0.050; Hofmann et al., 1986), and Eu/Eu* ratios of the seamount lavas are >1. Microscopic examination of the seamount glasses reveals rare, quench crystals of plagioclase in a few of the samples, but none of these samples contain plagioclase phenocrysts, therefore the high Sr/Nd, Pb/Ce and Eu/Eu* ratios of the seamount glasses cannot be the result of plagioclase accumulation. In addition, laser ablation ICP-MS analyses of the seamount glasses have confirmed their high Sr/Nd ratios (L. Danyushevsky, pers. comm. 2001).

Niu and O'Hara (2006) have argued that the most primitive MORB have Eu/Eu* >1, and that the depleted upper mantle therefore has a positive Eu anomaly that complements the negative anomaly of the bulk continental crust. The least evolved of the Group 1 axial lavas have Eu/Eu* >1, and Eu/Eu* decreases with decreasing MgO reflecting plagioclase fractionation (Fig. 7), but the seamount lavas are displaced above this array to higher Eu/Eu* and Sr/Nd than are typical of aphyric MORB.

Seamount lavas from dredges 5, 6 and 7 have higher $^{87}Sr/^{86}Sr$ and lower $^{143}Nd/^{144}Nd$ than the lavas from the ridge axis. Thus, although

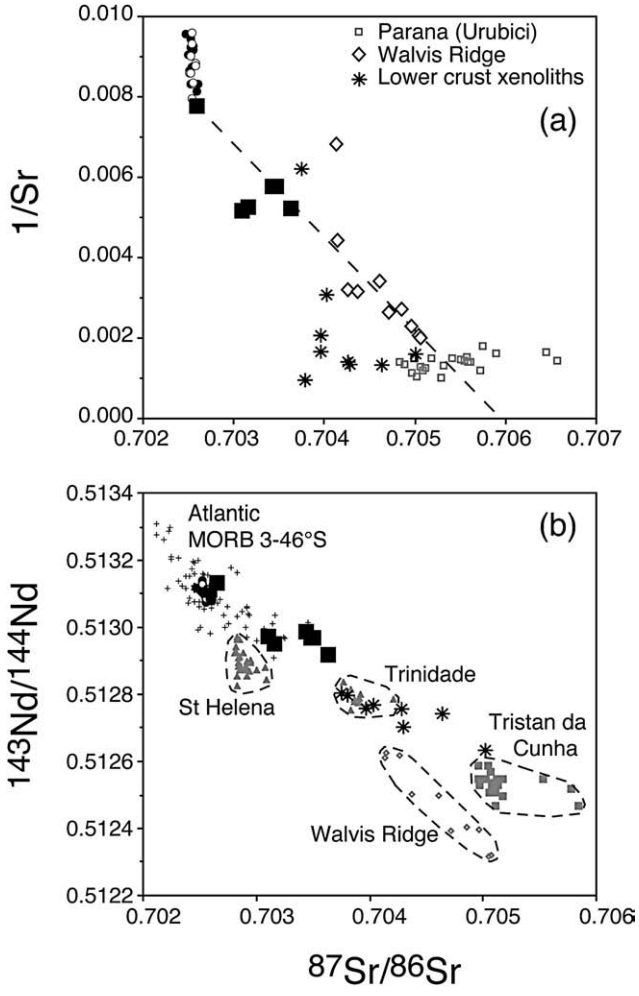


**Fig. 4.** Variation of $^{87}Sr/^{86}Sr$ with (a) 1/Sr, (b) $^{143}Nd/^{144}Nd$ for lavas from the MAR at 26°S. Dashed line in (a) indicates upper limit of 0.706 for high $^{87}Sr/^{86}Sr$ endmember, assuming mixing between a high $^{87}Sr/^{86}Sr$ component and an endmember with a composition similar to axial lavas. Data for Namibian lower crustal xenoliths, Walvis Ridge lavas, and Urubici Parana lavas in (a) are from Class and le Roex (2006), Richardson et al. (1982) and Peate et al. (1999) respectively. Data for the MAR between 3°S and 46°S (Fontignie and Schilling, 1996), and South Atlantic OIB (Richardson et al., 1982; Chaffey et al., 1989; le Roex et al., 1990; Halliday et al., 1995; Siebel et al., 2000) shown in (b) for comparison. 2$\sigma$ error bars are smaller than symbol size.

measured Rb/Sr ratios of the seamount lavas are lower than those of the axial lavas, the higher $^{87}Sr/^{86}Sr$ values of the seamount lavas indicate that they were derived from a source with time-integrated higher Rb/Sr, and are therefore likely to have undergone a relatively recent melt extraction event. Samples from dredges 1 (which is from a different ridge segment) and 10 have isotope compositions within the range of the axial lavas. Pb isotope data do not lie upon the linear arrays defined by the axial lavas. Instead, the seamount lavas have

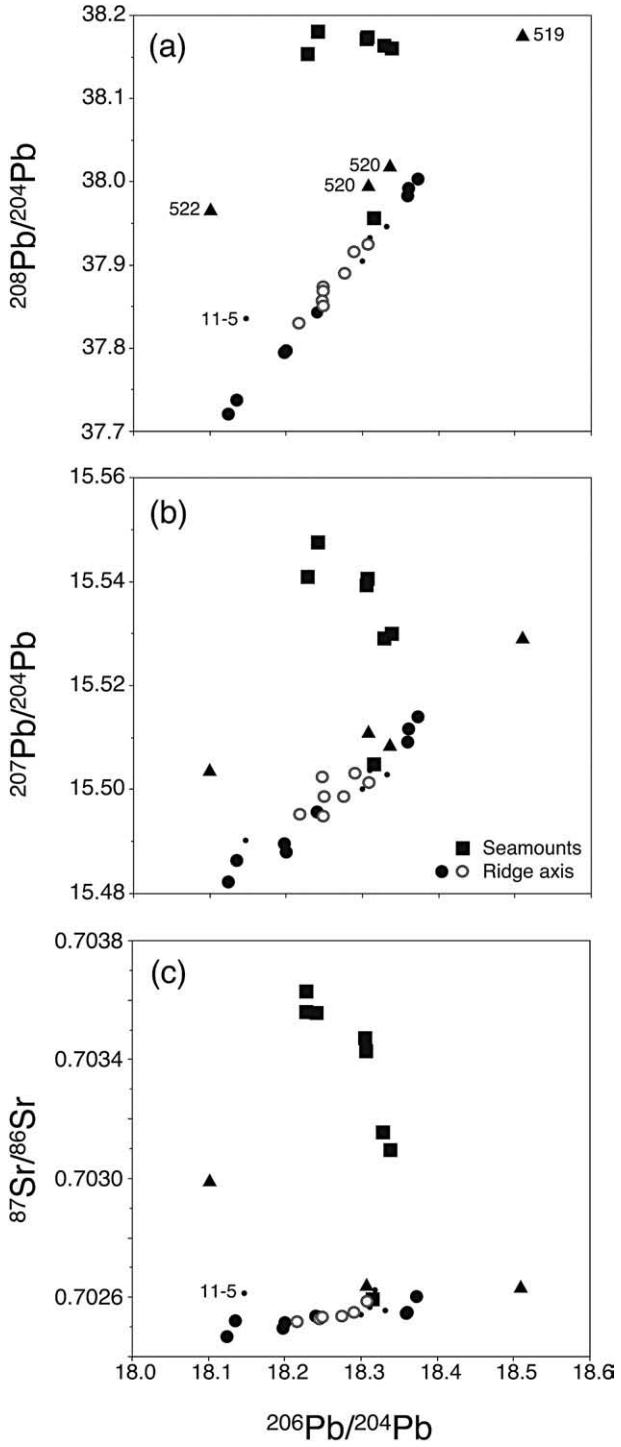


**Fig. 5.** Pb isotope compositions of the 26°S samples, measured using the triple-spike technique. 2$\sigma$ error bars are smaller than symbol size. Data for glasses from adjacent ridge segments (small black circles), and from older crust at DSDP Sites 519, 520, 522 (triangles) shown for comparison.

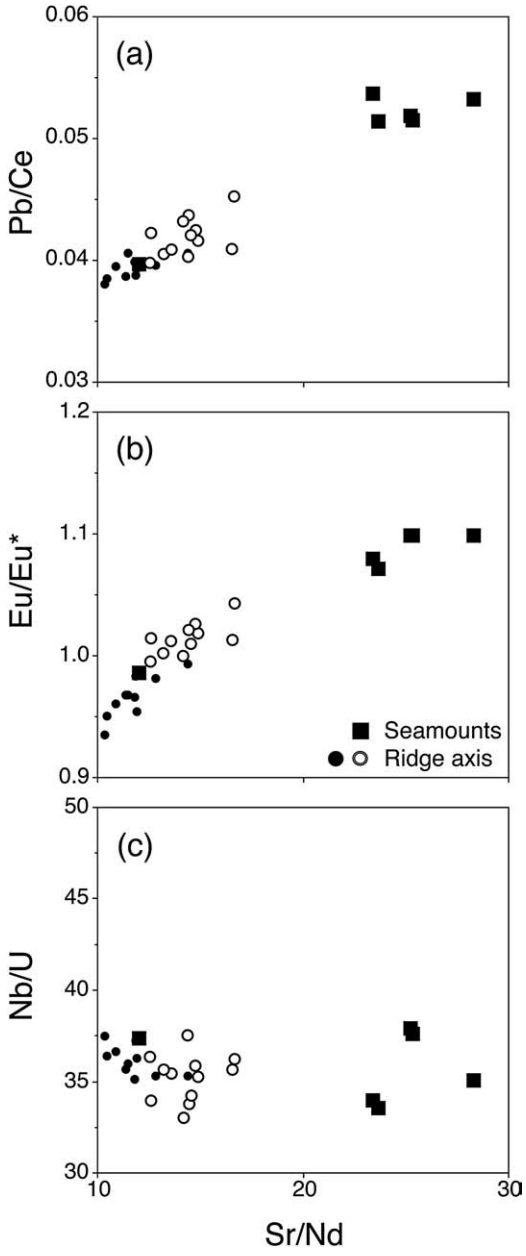


**Fig. 6.** Variation in Sr/Nd with (a) Pb/Ce, (b) Eu/Eu*, (c) Nb/U. Eu/Eu* is defined as $Eu_N/(Sm_N \times Gd_N)^{0.5}$, where N indicates chondrite-normalised abundances. Seamount lavas have Eu/Eu* > 1, and higher Pb/Ce and Sr/Nd ratios than lavas from the ridge axis.

higher $^{207}Pb/^{204}Pb$ and $^{208}Pb/^{204}Pb$ for a given $^{206}Pb/^{204}Pb$, and define an apparent negative correlation between $^{207}Pb/^{204}Pb$ and $^{206}Pb/^{204}Pb$ (Fig. 5). Graham et al. (1996) have shown that there is a highly significant positive correlation between $^{87}Sr/^{86}Sr$ and $^{3}He/^{4}He$ for the seamount lavas (Fig. 8). Our data show further that the seamount lavas with the highest $^{87}Sr/^{86}Sr$ and $^{3}He/^{4}He$ have the highest Sr/Nd and Eu/Eu*, and the lowest concentrations of highly and moderately incompatible elements (Fig. 8). At 26°S, the high $^{87}Sr/^{86}Sr$ component appears to be of limited extent; it occurs only in lavas from the seamount and related cones sampled by dredges 5, 6, 7, and is not present in lavas from the ridge axis. However, glasses from the MAR at 35–40°S close to Tristan da Cunha and Gough Islands have similarly high $^{87}Sr/^{86}Sr$ values (Fontignie and Schilling, 1996). These Atlantic seamounts differ from most Pacific near-ridge seamounts, which erupt lavas with trace element and isotope compositions that are both more enriched and more depleted than lavas from the nearby ridge axis (Niu and Batiza, 1997; Niu et al., 2002).

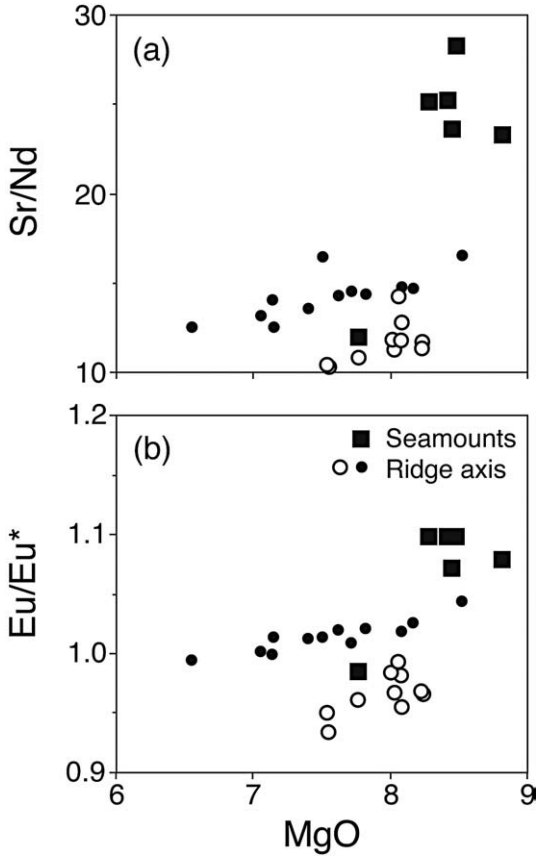


**Fig. 7.** Variation of Sr/Nd and Eu/Eu* with MgO for glasses from 26°S. Decreasing Sr/Nd and Eu/Eu* with decreasing MgO for axial lavas results from plagioclase fractionation. For a given value of MgO, seamount lavas have higher Sr/Nd and Eu/Eu* than axial lavas.

The geochemical differences between the lavas from the ridge axis and from nearby seamounts may be summarised as follows:

(a) In terms of incompatible trace elements, all samples are depleted N-MORB. Seamount lavas are more depleted in highly incompatible elements than axial lavas. Except for one sample (RC1-1), the seamount lavas have higher Pb/Ce, Sr/Nd and Eu/Eu* than axial lavas.
(b) Despite their lower Rb/Sr ratios, most seamount lavas have higher $^{87}Sr/^{86}Sr$ and lower $^{143}Nd/^{144}Nd$ than the axial lavas. Seamount lavas with the highest $^{87}Sr/^{86}Sr$ also have the highest $^{3}He/^{4}He$ and $^{208}Pb/^{206}Pb$, the highest Sr and Eu anomalies, and the lowest incompatible trace element concentrations.
(c) Samples from the ridge axis define linear arrays in triple-spike Pb–Pb isotope space, but seamount lavas are displaced from these arrays to higher $^{207}Pb/^{204}Pb$ and $^{208}Pb/^{204}Pb$ for a given $^{206}Pb/^{204}Pb$.

## 6. Discussion

### 6.1. Pb isotope systematics of lavas from the ridge axis

Lavas from the 26°S ridge segment define linear arrays in Pb isotope diagrams. Glasses from the MAR axis immediately to the north and south of the 26°S segment have Pb isotope compositions which overlap with those of glasses from 26°S, except for sample EN063 11D-5g (from north of the Rio Grande Transform), which is displaced to higher $^{208}Pb/^{206}Pb$ and $^{87}Sr/^{86}Sr$, and may reflect mixing with the material which contributes to the seamount lavas. The boundary between mantle with 'Tristan-like' (high $^{87}Sr/^{86}Sr$, low $^{206}Pb/^{204}Pb$) and 'St Helena-like' (low $^{87}Sr/^{86}Sr$, high $^{206}Pb/^{204}Pb$) isotopic characteristics, located at 24°S by Fontignie and Schilling (1996), must actually lie to the south of 26°S, although the presence of one high $^{208}Pb/^{206}Pb$ sample (EN063 11D-5g) to the north of the 26°S segment shows that

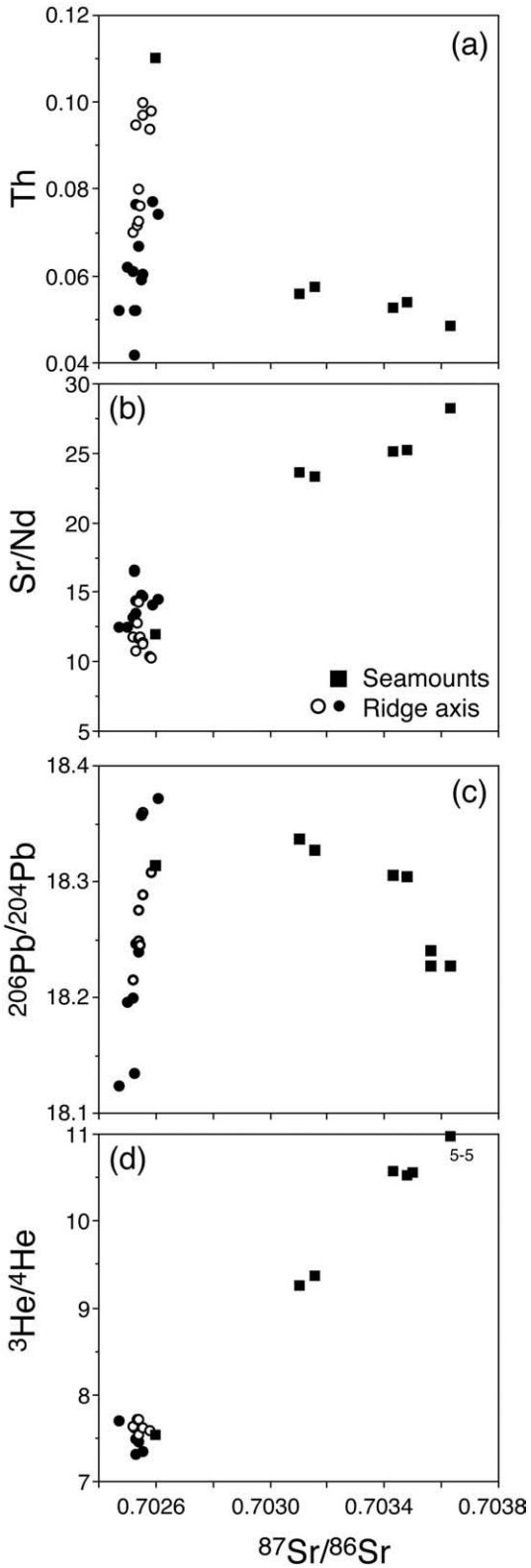


**Fig. 8.** Variation of $^{87}Sr/^{86}Sr$ with (a) Th, (b) Sr/Nd, (c) $^{206}Pb/^{204}Pb$, (d) $^{3}He/^{4}He$. Seamount lavas with the highest Sr/Nd and Eu/Eu* have the lowest incompatible element concentrations, the lowest $^{206}Pb/^{204}Pb$, and highest $^{87}Sr/^{86}Sr$ and $^{3}He/^{4}He$ ratios. Helium isotope data for the 26°S lavas are from Graham et al. (1996). $2\sigma$ error bars are smaller than symbol size.

the boundary is not sharply defined. Four glass samples from DSDP Sites 519, 520 and 522 do not lie on the arrays defined by the axial lavas, and possibly reflect a decreasing role with time for a component with high $^{208}Pb/^{204}Pb$ for a given $^{206}Pb/^{204}Pb$ (Fig. 5).

A sample of Fe–Mn oxyhydroxide coating removed from sample RC7-4 (Table 2) has a relatively radiogenic Pb isotope composition which is probably close to that of local seawater, and does not lie on an extension of the array defined by the samples from the ridge axis, indicating that variable alteration cannot explain the Pb isotope array defined by the glasses from the ridge axis.

The slope of the axial data in the $^{206}Pb/^{204}Pb$–$^{207}Pb/^{204}Pb$ diagram, if interpreted as an isochron, yields an age of ~1.92 Ga. The fact that the data also define a linear array in the $^{206}Pb/^{204}Pb$–$^{208}Pb/^{204}Pb$ diagram indicates that either the $\kappa$ value ($^{232}Th/^{238}U$) of the source is the same for all samples, or that $\kappa$ varies linearly with $\mu$ (White et al., 1987). For a source age of 1.92 Ga, the slope of the data in the $^{206}Pb/^{204}Pb$–$^{208}Pb/^{204}Pb$ diagram implies a source Th/U of ~4.0, which is about twice the Th/U ratios measured in the lavas themselves (1.8–2.2), and higher than source Th/U ratios inferred from Th isotope ratios in zero-age lavas from the 33°S segment on the MAR (0.8–0.9; Lundstrom et al., 1998). Thus unless the source of the axial lavas underwent a melt depletion event which decreased Th/U, recently enough that Pb isotope compositions were unaffected, the Pb isotope arrays are unlikely to represent isochrons.

Two component mixing is a more likely explanation for the data arrays in Fig. 5. The ridge axis lavas with the most radiogenic Pb isotope compositions tend to have higher concentrations of incompatible elements, and higher ratios of more- to less-incompatible elements such as Nb/Zr, Th/La (not shown), which is consistent with an origin by two component mixing. Hanan et al. (1986) and Fontignie and Schilling (1996) suggest that the isotope compositions of MORB from the MAR between 5° and 27°S result from mixing of depleted upper mantle with material from the Saint Helena plume. However, an extension of the 26°S triple spike data does not pass through the field for Saint Helena lavas in Fig. 9a. If the Pb isotope arrays in Fig. 5 are indeed two-component mixing lines, the high $^{206}Pb/^{204}Pb$ endmember could be mantle with a composition similar to that underlying the island of Trinidade, which is the nearest intraplate volcanic island in terms of latitude (Fig. 1), but is located ~1700 km west of the MAR axis. On the other hand, the Pb–Sr isotope systematics of the 26°S axis lavas are not easily explained by such mixing (Fig. 9c).

The linear Pb isotope arrays might result from mixing of melts within crustal level magma chambers. However, Group 1 lavas, most of which are from the magmatically robust, central part of the ridge segment at 26°S (Fig. 2) have more variable Pb isotope compositions than the Group 2 lavas from the segment ends (Fig. 5), where magma chambers are likely to be smaller and less continuous. This suggests that the mixing may take place within the mantle, due to mixing of sources, or mixing during the melting process.

### 6.2. Role of mixing in controlling compositions of seamount lavas

The apparent negative correlation of $^{207}Pb/^{204}Pb$ with $^{206}Pb/^{204}Pb$ for the seamount lavas (Fig. 5b) is difficult to explain by any process other than mixing. $^{206}Pb/^{204}Pb$ correlates negatively with $^{87}Sr/^{86}Sr$ and Sr/Nd, (Fig. 5c, 8c) which implies that the correlations of isotope ratios with trace element compositions within the seamount lavas (Fig. 8) are most likely the result of mixing between a component with similar composition to lavas from the ridge axis, and an endmember with higher Sr/Nd, Pb/Ce, $^{87}Sr/^{86}Sr$ and $^{3}He/^{4}He$ than the most extreme seamount sample RC5-5. An upper limit of about 0.706 for the $^{87}Sr/^{86}Sr$ ratio of the high Sr/Nd endmember can be obtained from the intercept of the data array with the y axis in Fig. 4a — this value is similar to that inferred for the enriched component in Walvis Ridge lavas by Richardson et al. (1982). In addition, the curvature of mixing arrays in diagrams such as Fig. 8 can be used to place constraints on the relative concentrations of trace elements in both mixing endmembers. For example, Graham et al. (1996) pointed out that the linear array of data in the $^{87}Sr/^{86}Sr$–$^{3}He/^{4}He$ diagram (Fig. 8) implies that the $^{86}Sr/^{4}He$ ratio of the two mixing endmembers must be similar. Since the high $^{206}Pb/^{204}Pb$ mixing endmember is similar in composition to the lavas from the ridge axis, the mixing event responsible for the range in

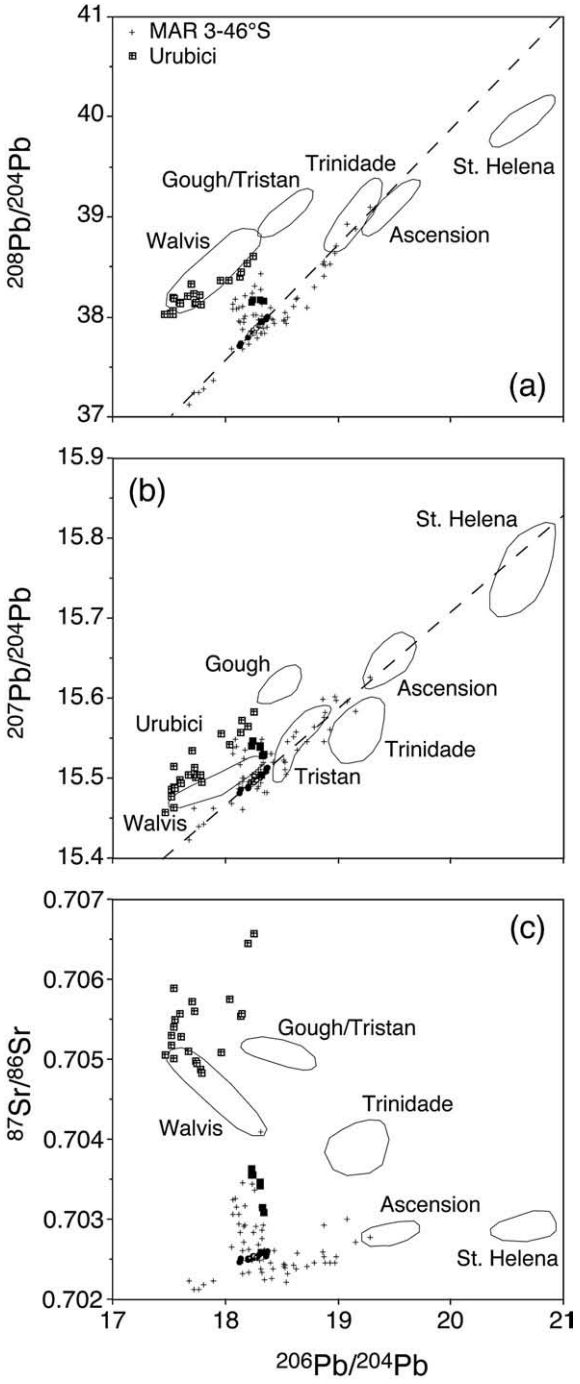


**Fig. 9.** Variation of (a) $^{208}Pb/^{204}Pb$, (b) $^{207}Pb/^{204}Pb$ and (c) $^{87}Sr/^{86}Sr$ with $^{206}Pb/^{204}Pb$ for lavas from the Mid-Atlantic Ridge between 3 and 46°S, the Walvis Ridge and Rio Grande Rise, Tristan da Cunha and Gough Islands, and the Parana flood basalt province (Urubici magma type). Pb isotope data are uncorrected for U, Th decay since eruption. Data from Peate et al. (1999), le Roex et al. (1990), Richardson et al. (1982), Gibson et al. (2005), Hanan et al. (1986), Fontignie and Schilling (1996). 2$\sigma$ error bars are smaller than symbol size.

composition of the seamount lavas must postdate that responsible for the Pb isotope arrays observed in the axial lavas.

### 6.3. Gabbro assimilation not responsible for compositions of seamount lavas

The high Sr/Nd, Pb/Ce, Eu/Eu* and low $CaO/Al_2O_3$ ratios of the seamount lavas might be the result of assimilation of plagioclase or plagioclase-rich cumulates within the oceanic lithosphere by 'normal', ridge axis magmas. Assimilation of gabbro has been invoked to explain incompatible element depleted, Sr- and Eu-enriched lavas from Iceland (Hémond et al., 1993) and from the Kerguelen Plateau (Yang et al., 1998), and melt inclusions in olivines from lavas from the Siquiros Transform (Danyushevsky et al., 2001).

The seamount lavas with the highest Sr/Nd and Eu/Eu* ratios also have the lowest incompatible trace element concentrations (Fig. 8). These inverse correlations are the opposite to those expected for assimilation-fractional crystallisation involving oceanic gabbro, but might be explained if variably-depleted seamount magmas had assimilated approximately similar amounts of altered gabbro containing cumulate plagioclase. This process would have the greatest effect on the most depleted magmas, which would then have the highest Sr/Nd, Eu/Eu*, and would have least influence on the ratios of incompatible elements which have low concentrations in gabbro, such as Nb/U. On the other hand, assimilation of gabbros by variously depleted magmas would be unlikely to result in the observed good correlations between trace element and isotope ratios (Fig. 8).

In addition, large amounts of gabbro assimilation are required to explain the high Sr/Nd ratios of the seamount lavas. For example, assuming a contaminant with Sr/Nd of 80 and a Sr concentration of 160 ppm (Hart et al., 1999) would require ~40% assimilation to account for the range in Sr/Nd in the seamount lavas. Gabbro assimilation also does not fully explain the trace element compositions of the seamount lavas. Ba and Sm are less incompatible in plagioclase than Nb and Hf respectively, and gabbros containing cumulate plagioclase have relatively high Ba/Nb and Sm/Hf (Fig. 10). In contrast, the seamount lavas have lower Ba/Nb and Sm/Hf than lavas from the ridge axis, unlike other lavas which have apparently assimilated gabbro (e.g. Saal et al., 2007). Although melt percolation through gabbro matrix can yield Sr and Eu enriched melts lacking Ba enrichment (Gurenko and Sobolev, 2006), this process imparts negative Zr, Hf anomalies to the melts, which are not observed in the seamount glasses (Fig. 10). Most oceanic gabbros have highly variable Ba/Rb ratios due to interaction with seawater and plagioclase accumulation (Hart et al., 1999; Coogan et al., 2001), but the seamount lavas have similar Ba/Rb ratios to unaltered oceanic basalts (Fig. 3).

The isotopic compositions of the seamount lavas are also not readily explained by assimilation of oceanic gabbro. $^{87}Sr/^{86}Sr$ ratios of the seamount lavas are higher than those of South Atlantic MORB. Altered gabbros that have been contaminated with seawater Sr could have suitable Sr isotope compositions, but young oceanic gabbros which have interacted with seawater will be displaced to the high $^{87}Sr/^{86}Sr$ side of the Sr–Nd mantle array (Hart et al., 1999), whereas the seamount lavas also have relatively low $^{143}Nd/^{144}Nd$, and lie close to the mantle array in Fig. 4. Assimilation of 'normal' oceanic gabbro also does not explain the relatively high $^{3}He/^{4}He$ and $^{208}Pb/^{204}Pb$ ratios of the seamount lavas.

In conclusion, the enrichments in Sr, Pb and Eu, and the depletions in highly incompatible elements such as Ba and Rb in the seamount lavas, cannot be the result of assimilation of plagioclase-rich cumulates by magmas within the oceanic crust, and must therefore be inherited from their mantle source.

### 6.4. Recycled oceanic gabbro in the source of seamount lavas?

High Sr/Nd ratios in lavas from some intraplate islands have been interpreted as evidence for recycled oceanic gabbro in the form of

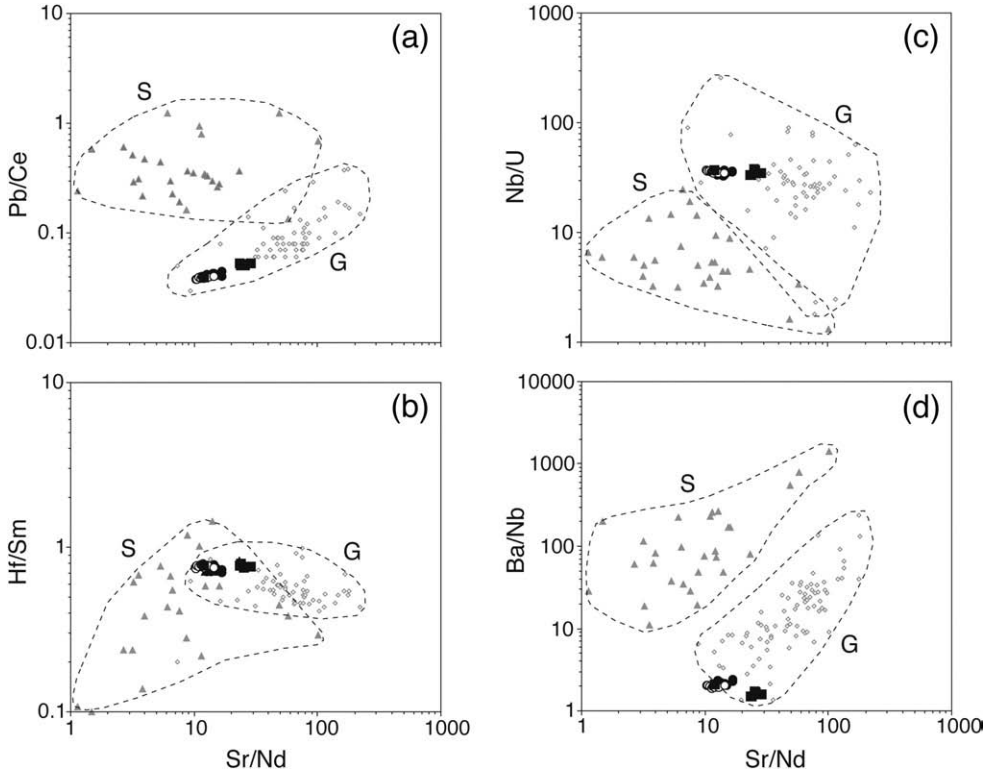


**Fig. 10.** Trace element compositions of lavas from the MAR at 26°S, with data for oceanic gabbros (G) and sediments (S) for comparison. The 26°S seamount lavas have low Ba/Nb and high Hf/Sm compared to most oceanic gabbros, and high Sr/Nd, Hf/Sm and low Ba/Nb compared to oceanic sediments. The trace element compositions of the seamount lavas are therefore difficult to explain by assimilation of oceanic gabbros, or by recycling of gabbro or oceanic sediments. Trace element data for oceanic gabbros from Hart et al. (1999) and Coogan et al. (2001). Oceanic sediment data are weighted average subducting compositions of Plank and Langmuir (1998).

eclogite, within the mantle source of these lavas (Hofmann and Jochum, 1996; Chauvel and Hémond, 2000; Sobolev et al., 2000). Gasperini et al. (2000) suggest that melting of recycled gabbro from subducted oceanic plateaus may explain the enrichments in Sr, Eu, Pb and Ba in basalts from Sardinia.

However, as discussed above, the incompatible trace element compositions of the seamount lavas, in particular their low Ba contents, relatively low Ba/Nb, high Hf/Sm (Fig. 10) and uniform Rb/Ba ratios (Fig. 3), are not easily explained by a contribution from oceanic gabbro. The isotopic compositions of the seamount lavas are also inconsistent with the presence of ancient, recycled gabbro in their source. Oceanic gabbros have low Rb/Sr, U/Pb, Th/Pb and Th/U ratios (Hart et al. 1999), which over time will result in relatively unradiogenic Sr and Pb (Stracke et al., 2003). The seamount lavas have high $^{208}Pb/^{206}Pb$ (time-integrated high Th/U), and high $^{87}Sr/^{86}Sr$ ratios, compared to the lavas from the ridge axis, unlike the predicted compositions of recycled gabbro. In addition, the seamount lavas have relatively unradiogenic He, but oceanic crustal rocks are likely to have higher $U/^{3}He$ than the mantle and over time will develop lower $^{3}He/^{4}He$ (e.g. Moreira and Kurz, 2001).

### 6.5. Recycled pelagic sediment?

The trace element and isotopic characteristics of some EM-1 type lavas from the Atlantic have been attributed to melting of a mantle source containing a small amount of ancient subducted pelagic sediment (Weaver et al., 1987; Andres et al., 2002). Many pelagic sediments have low $^{238}U/^{204}Pb$, and ancient subducted sediments may therefore evolve to low $^{206}Pb/^{204}Pb$, low $^{143}Nd/^{144}Nd$ and high $^{87}Sr/^{86}Sr$ (e.g. Stracke et al., 2003). However, ancient sediment will have $^{208}Pb/^{204}Pb$ ratios that are lower than those of the depleted upper mantle, whereas the seamount lavas have higher $^{208}Pb/^{204}Pb$ than lavas from the nearby ridge axis.

Average subducting sediment has a Sr/Nd ratio of 12 (Plank and Langmuir, 1998), which is too low to account for the high Sr/Nd ratios of the seamount lavas (Fig. 10). Although some carbonate-rich sediments have the required high Sr/Nd, these also have high Ca/Al, whereas the seamount lavas have low Ca/Al. Most continent-derived sediments have high Pb/Ce and low Nb/U ratios due to the preferential transfer of Pb and U to the continents by fluids at subduction zones. Although the seamount lavas have high Pb/Ce, they have Nb/U ratios that are similar to those of lavas from the ridge axis. Many pelagic sediments have lower Hf/Sm than MORB, because they lack detrital zircon, but the seamount lavas have higher Hf/Sm than lavas from the adjacent ridge axis (Fig. 10). In addition, the seamount lavas have lower Ba/Nb ratios than lavas from the ridge axis, whereas sediments are characterised by high Ba/Nb. Thus, unlike sediments, the seamount lavas have relatively high HFSE/LILE and HFSE/REE ratios.

### 6.6. Lower continental crust in the South Atlantic upper mantle

We suggest that the distinctive trace element and isotopic compositions of the seamount lavas result from melting of a mantle source contaminated with lower continental crustal material. As discussed above, the trace element compositions of the seamount lavas show that a plagioclase-rich component contributed to the source of the seamount lavas. Basaltic liquids do not reach saturation in plagioclase at pressures of >1 GPa (35–45 km, below the continental Moho), suggesting that at one stage, the material carrying the high Sr/Nd signature existed at crustal depths. The major element compositions of the seamount lavas indicate that they were formed by smaller degrees of melting at greater depth, compared to the lavas from the adjacent ridge axis (Batiza et al., 1989). In crustal material transported to mantle depths, plagioclase will have been replaced by recrystallisation, but in a closed system the trace element characteristics of plagioclase will remain.

Plagioclase is known to be an important phase in the lower continental crust (LCC), where it is concentrated as a result of intra-crustal differentiation (e.g. Rudnick, 1995; Rudnick and Gao, 2003). As a result, the LCC has high Sr/Nd, Pb/Ce, and a positive Eu anomaly relative to depleted upper mantle (Rudnick and Fountain, 1995; Rudnick and Gao, 2003). The LCC also has higher Nb/U, but generally much lower Nb and U concentrations (due to the presence of melting residues and/or cumulates) than the bulk or upper continental crust, which could explain why the seamount lavas have Nb/U ratios within the range of mantle-derived lavas, but elevated Pb/Ce.

The lower continental crust has low U/Pb, Th/Pb compared to the upper continental crust and upper mantle, and has lower Rb/Sr than the upper continental crust (Zartman and Haines, 1988; Taylor and McLennan, 1985; Kramers and Tolstikhin, 1997; Rudnick and Gao, 2003). Old lower continental crust will therefore develop unradiogenic Pb and moderately radiogenic Sr, and such compositions are in fact characteristic of many lower crustal xenoliths.

There are few data that constrain the composition of the lower crust on the South Atlantic continental margins. Class and le Roex (2006) reported Sr and Nd isotope data for xenoliths from the lower crust and lithospheric mantle from the Damara Belt of northern Namibia. The lower crustal xenoliths have present day $^{87}Sr/^{86}Sr$ ratios of 0.7038 to 0.7050 and high Sr/Nd ratios (up to 200), and the most radiogenic of these lie on an extension of the $^{87}Sr/^{86}Sr$–1/Sr array in Fig. 4a. Although Pb isotope data are not available for these samples, many lower crustal rocks worldwide do have suitable Pb isotope compositions (see compilation in Meyzen et al., 2005). Assuming that the Damara Belt xenoliths are representative of the local lower continental crust, <10% LCC is required to explain the range in $^{87}Sr/^{86}Sr$ observed in the seamount lavas. Although high $^{3}He/^{4}He$ ratios are apparently inconsistent with a contribution from continental material, some lower crustal granulites (which have very low U concentrations) contain pure mantle He (Dunai and Touret, 1993). It is also possible that the source of the seamount lavas was more recently enriched in unradiogenic mantle He by diffusion (Albarède, 2008), after it was incorporated into the mantle.

Several previous studies have concluded that remnants of lower continental crust may be present in the upper mantle beneath the South Atlantic. Escrig et al. (2005) showed that the Os, Pb and Sr isotope compositions of some MORB glasses from the southernmost MAR are best explained by the presence of lower continental crust in their mantle source. Kamenetsky et al. (2001) showed that the composition of one anomalous MORB glass with high $^{87}Sr/^{86}Sr$, high Pb/Ce and low $^{206}Pb/^{204}Pb$ from the MAR at 54.4°S was consistent with the presence of LCC in the upper mantle. In the Indian Ocean, a component derived from the LCC has been proposed to explain the compositions of lavas with Dupal characteristics from spreading centres (Mahoney et al., 1992; Hanan et al., 2004; Janney et al., 2005; Meyzen et al., 2005), and intraplate oceanic volcanoes (Mahoney et al., 1996; Borisova et al., 2001; Frey et al., 2002).

### 6.7. Regional distribution of continental material in the South Atlantic mantle

Lavas with Dupal-like isotope compositions are widespread in the southern Atlantic, and occur in a range of tectonic settings, including the mid-ocean ridge system, intraplate oceanic islands, as well as the Parana–Etendeka continental flood basalt province and related intrusions associated with the rifting of Africa from South America.

The South Atlantic Dupal Anomaly as mapped by Hart (1984) is centered on latitudes 30–45°S. Fontignie and Schilling (1996) showed that MORB from the MAR south of about 24°S have relatively high $^{208}Pb/^{204}Pb$ for a given $^{206}Pb/^{204}Pb$, and extend towards the field for lavas from Tristan da Cunha in Fig. 9. These axial lavas thus contain a 'dilute' expression of the high $^{208}Pb/^{204}Pb$, high $^{87}Sr/^{86}Sr$ component observed in the seamount lavas from 26°S. Lavas from the MAR at 36–

38°S, directly to the west of Tristan da Cunha, have $^{87}Sr/^{86}Sr$ values of up to 0.704, and are inferred to result from recent, westward, channelled flow of more enriched mantle material from beneath Tristan da Cunha to the ridge axis immediately to the west (Fontignie and Schillling, 1996; Humphris et al., 1985). Sr and Pb isotope compositions of these lavas overlap with those of the seamount lavas (Fig. 9).

The intraplate Rio Grande Rise and Walvis Ridge are generally thought to have formed due to melting above a mantle plume now situated beneath Tristan da Cunha. Most lavas from these locations have Dupal-like compositions, however in detail lavas display a wide range in compositions, and require the presence of several different endmember compositions which are mixed together in varying proportions (Humphris and Thompson, 1982; Richardson et al., 1982; Gibson et al., 2005). Lavas from DSDP Site 525 on the Walvis Ridge and Site 516 on the Rio Grande Rise have lower $^{206}Pb/^{204}Pb$ and higher $^{87}Sr/^{86}Sr$ ratios than the lavas recovered from other sites on this aseismic ridge system. Lavas from Tristan da Cunha (and Inaccessible and Gough Islands) have incompatible trace element and isotope compositions which overlap with those of lavas from the Walvis Ridge, but extend to more radiogenic Pb isotope compositions (Fig. 9).

Plate reconstructions show that the Parana–Etendeka continental flood basalts, which were erupted at ~134 Ma at the time of rifting of South America and Africa, formerly overlay the region of upper mantle which now defines the Dupal Anomaly. Hawkesworth et al. (1986) showed that many of these lavas are also characterised by extreme Dupal-type compositions. For example, the flood basalts showing the least evidence for upper-crustal contamination (the Urubici magma type of Peate et al., 1999) have relatively high $^{208}Pb/^{204}Pb$ and $^{207}Pb/^{204}Pb$ and low $^{206}Pb/^{204}Pb$ (Hawkesworth et al., 1986; Peate et al., 1999; Fig. 9). The Sr, Nd and Pb isotope compositions of these flood basalts overlap with those of lavas from Site 525 on the Walvis Ridge, and are very similar to those inferred for the high Sr/Nd component in the seamount lavas (Fig. 9). The Parana lavas are all relatively evolved (MgO 3–5%) and have fractionated substantial amounts of plagioclase, which will have affected their Sr/Nd, Pb/Ce and Eu/Eu* ratios. Nevertheless, the similarity between the Pb isotope compositions of these lavas and that inferred for the high $^{87}Sr/^{86}Sr$ component in the 26°S MAR seamount lavas as well as lower crustal xenoliths, suggests that the latter contributes to flood basalt magmatism.

The unusual compositions of young lavas from this region of the South Atlantic are most likely the result of continental material in the upper mantle, either in the form of continental crust or lithospheric mantle (Hawkesworth et al., 1986; Douglass et al., 1999; Gibson et al., 2005; Class and le Roex, 2006). However, the mechanism by which this continental material was introduced into the upper mantle is currently debated. Castillo (1988), Peate et al. (1999) and Gibson et al. (2005) suggested that at least some of this continental material is introduced into the upper mantle from depth by mantle plumes. In contrast, Hawkesworth et al. (1986) argued that the Dupal anomaly represents a relatively shallow feature of the mantle, resulting from remobilisation of continental lithospheric mantle during flood basalt magmatism and continental breakup in the South Atlantic at 132 Ma. It is also possible, as proposed by Class and le Roex (2006), that continental material recently detached from the Gondwanaland lithosphere during rifting in the South Atlantic has been entrained into a mantle plume beneath Tristan. Douglass et al. (1999) suggest that lavas with continental geochemical characteristics are only associated with intraplate magmatism in the South Atlantic because the continental lithospheric mantle that is dispersed into the convecting upper mantle during rifting is relatively refractory, and therefore contributes to magmatism only where mantle temperatures are higher than normal. Our results show that fragments of lower continental crust have also been dispersed in the upper mantle in this region. The mixing relationships discussed earlier indicate that this material was introduced into the upper mantle relatively recently, most likely during continental rifting, and probably does not represent deeply-recycled lower continental crust. This suggests that the Dupal Anomaly is of relatively recent origin (dating from the time of continental breakup), and restricted to the upper mantle. The discovery of Palaeozoic/Proterozoic zircons in young gabbros from the northern MAR (Pilot et al., 1998) indicates that at least beneath the North Atlantic, continental material has been introduced into the upper mantle relatively recently, rather than having been recycled through the deep mantle by mantle plumes.

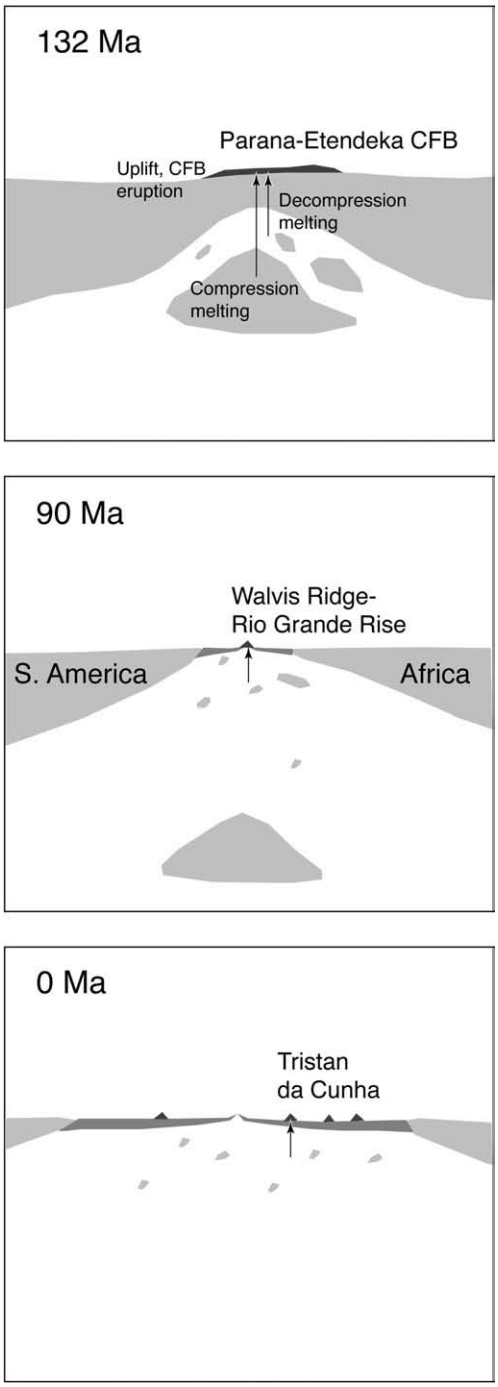


**Fig. 11.** Cartoon, not to scale, illustrating breakup of South Atlantic and subsequent intraplate magmatism. Arrows show direction of melt transport. At 134 Ma, delamination of lower crust resulting from rifting leads to eruption of flood basalt magmas, derived partly from sinking lower crust by compression melting. Remnants of crust and lithospheric mantle in the upper mantle contribute to subsequent oceanic magmatism in the region of the South Atlantic Dupal Anomaly.

### 6.8. Crustal delamination, flood basalt magmatism, and the creation of Dupal mantle

One way of introducing lower continental crust into the upper mantle is by delamination. Delamination has been invoked to explain regions of high continental heat flow, rapid regional uplift, and some intraplate continental volcanism. It is indirectly inferred to be responsible for the andesitic composition of the bulk crust (e.g. Taylor and McLennan, 1985; Rudnick, 1995), and for creating heterogeneity in the mantle (Arndt and Goldstein, 1989; Tatsumi, 2000). We suggest that delamination during continental rifting was responsible for introducing continental material into the South Atlantic mantle, and speculate that this process may also have been the cause of flood basalt magmatism (Fig. 11).

Models for the generation of flood basalts must be capable of generating large volumes of melt relatively rapidly. There are several ways in which delamination of lower continental crust might result in melting (Anderson, 2005, 2006; Elkins-Tanton and Hager, 2000; Lustrino, 2005; Hales et al., 2005; Kay and Kay, 1993; Arndt and Goldstein, 1989), namely (1) decompression melting of mantle upwelling to take the place of the sinking crustal material; (2) warming and melting of the delaminated crustal material; (3) melting of the sinking lower crust due to pressure increase, or 'compression melting' (Niu, 2005). Of these mechanisms, (1) and (3) are likely to result in a close association in time between rifting (assuming that rifting triggers crustal detachment) and magmatism (Fig. 11), as is observed in the South Atlantic (Renne et al., 1992; Turner et al., 1994). On the other hand, (1) predicts that magma generation occurs mainly within the upper mantle, whereas (2) and (3) predict that magmas are derived at least in part from the sinking lower crustal material. Melting of sinking dense crustal material as a result of pressure increase (3) might therefore best explain rapid generation of large volumes of melt bearing a strong crustal signature. Niu (2005) pointed out that increase of pressure with little or no increase in temperature may result in melting of materials with negative solidus slope in the P–T diagram. Depending on the rate of delamination and the composition of the lower crust (e.g. volatile content), 'compression melting' may be a possible mechanism of generating large volumes of melt with crustal trace element and isotope characteristics relatively rapidly. Melting may also be enhanced by heating as the lower crustal material continues to sink into the upper mantle (Fig. 11).

As discussed above, the Parana lavas which have undergone the least contamination within the upper continental crust have strongly 'crustal' trace element and isotopic signatures (Peate et al., 1999). These geochemical characteristics are often assumed to be derived from the subcontinental lithospheric mantle (SCLM), which has often been invoked as a source of CFB, including the Parana–Etendeka (e.g. Hawkesworth et al., 1988). Nevertheless, the role of SCLM in flood basalt petrogenesis has been questioned (Arndt and Christensen, 1992; Menzies, 1992; Anderson, 1994), because the SCLM is relatively cool and refractory and is unlikely to melt to the extent required by flood basalt volumes, unless it is hydrous (Gallagher and Hawkesworth, 1992). However, there is little evidence that either the SCLM or the least evolved flood basalt magmas contain significant amounts of water (Arndt and Christensen, 1992). In addition, few xenoliths from the SCLM have the depletions in Nb and Ta relative to elements of similar incompatibility that are characteristic of many CFB (McDonough, 1990; Arndt and Christensen, 1992). On the other hand, the trace element and Sr–Pb–Os isotope compositions of flood basalts have been used to argue that lower continental crust, rather than lithospheric mantle was involved in their genesis (Peng et al., 1994; Chesley and Ruiz, 1998). Relatively large volumes of crust are required however (up to 40%), and so melting of mafic lower crust at mantle depths may be an attractive alternative to crustal level contamination.

The association of flood basalt magmatism in space and time with continental rifting, both in the South Atlantic and in many other CFB provinces, suggests that rifting may trigger delamination. Eclogites and garnet granulites in the lower continental crust are likely to be significantly denser than underlying peridotite, and can thus readily founder into the mantle during rifting (Arndt and Goldstein, 1989; Elkins-Tanton, 2005; Anderson, 2005, 2006). Crustal detachment and flood basalt magmatism tend to be localised at certain points along a passive margin. Foundering of lower crust into the mantle may only be possible if the underlying, less dense lithospheric mantle is removed, which may occur either by thinning during rifting (Anderson, 1994), or by 'thermal erosion' by plumes. Melt injection above a plume may also increase the density of the overlying lithosphere, leading to delamination (Elkins-Tanton and Hager, 2000; Elkins-Tanton, 2005; Deng et al., 2007).

Finally, delamination of dense lower continental crust is predicted to result in significant surface uplift. Gallagher et al. (1994) used apatite fission track data to argue that more than 2.5 km of uplift occurred along the coastal escarpment of southern Brazil, and detailed geochemical mapping of individual flood basalt flows in this area (Peate et al., 1999) suggests that much of this uplift occurred during and after flood basalt magmatism. In contrast, the initiating plume model for CFB magmatism would predict uplift prior to magmatism (Hill et al., 1992), and more precise constraints on the relative timing of uplift, rifting and magmatism in the South Atlantic could be used to test this hypothesis.

## 7. Conclusions and wider implications

### 7.1. Shallow, young origin for some upper mantle heterogeneity

Our data suggest that the Dupal signature in some lavas from the South Atlantic has a shallow origin in lower continental crust. Although the suggestion that continental material is responsible for the unusual isotope compositions of lavas from the South Atlantic is not new (e.g. Hawkesworth et al., 1986; Milner and le Roex, 1996; Peate et al., 1999; Gibson et al., 2005; Class and le Roex, 2006), many previous studies have assumed that this material is supplied from depth by mantle plumes. In contrast, our data suggest that the Dupal Anomaly is a relatively young, shallow feature of the South Atlantic mantle.

### 7.2 . Similar origin for other EM1

Some other intraplate lavas defined as EM1 on the basis of radiogenic isotope data have similar trace element systematics to the seamount lavas, in particular high Sr/Nd, Eu/Eu*, and Pb/Ce (Lustrino and Dallai, 2003). Lower continental crust may be widely introduced into the mantle during continental rifting, and may be responsible for some of the trace element and isotopic heterogeneity of the upper mantle. At least one other site of EM1 magmatism (Kerguelen) is known to be underlain by a detached fragment of lower continental crust (Frey et al., 2002). Arndt and Goldstein (1989), Tatsumi (2000) and Willbold and Stracke (2006) have previously suggested that lower continental crust may be the source of the distinctive isotopic compositions of EM1 lavas.

### 7.3. Crustal delamination responsible for CFB magmatism

If recently-introduced lower continental crust is responsible for the low $^{206}Pb/^{204}Pb$ signature of lavas from the Dupal Anomaly, then it is possible that the Parana–Etendeka flood basalts, many of which have extreme Dupal signatures, may have a relatively shallow (crustal) origin, rather than resulting from initiation of deep, hot, mantle plumes. We suggest that delamination of the lower continental crust may result in magmatism, either by allowing rapid upwelling of deeper asthenosphere, or by melting of the sinking crustal material (Elkins-Tanton and Hager, 2000; Anderson, 2005;

Hales et al., 2005; Lustrino, 2005; Niu, 2005). The 'continental' trace element and isotope compositions of the least contaminated flood basalts can then be explained without recourse to large (up to 40%) degrees of assimilation of crust. The amount of melt generated by this process need not be directly controlled by the lithospheric stretching factor $\beta$. Foundering of lower continental crust is normally prevented by the underlying,relatively depleted, physically buoyant mantle lithosphere. However, during continental riftingthe lithosphereis removed, allowing crustal delamination to take place. Continental rifting may therefore be the main plate tectonic process responsible for delamination of lower continental crust, which is inferred to drive the composition of the bulk crust towards more silicic, incompatible trace element enriched compositions (Rudnick, 1995).

## Acknowledgments

Rodey Batiza supplied the samples from the MAR at 26°S, and Jean-Guy Schilling kindly sent us basaltic glasses dredged during the 1981 EN063 (Endeavor) cruise. Glass samples from DSDP Leg 73 were provided by the Ocean Drilling Program (ODP). We thank Alan Greig for help with the trace element measurements, and Steve Galer for advice with the Pb triple spike analyses. Leonid Danyushevsky sent us unpublished LA-ICPMS trace element data for some of the seamount samples for comparison, and Nancy Grindlay kindly provided the bathymetric map of the 26°S segment (Fig. 2). M.R. thanks Al Hofmann for discussions and ideas, and David Graham, Dave Peate and an anonymous reviewer for reviews of various versions of this manuscript, part of which was written whilst the first author was at the University of Bristol.

## References

Albarède, F., 2008. Rogue mantle helium and neon. Science 319, 943–945.
Anderson, D.L., 1994. The sublithospheric mantle as the source of continental flood basalts; the case against the continental lithosphere and plume head reservoirs. Earth and Planetary Science Letters 123, 269–280.
Anderson, D.L., 2005. Large igneous provinces, delamination, and fertile mantle. Elements 1, 271–275.
Anderson, D.L., 2006. Speculations on the nature and cause of mantle heterogeneity. Tectonophysics 416, 7–22.
Andres, M., Blichert-Toft, J., Schilling, J.-G., 2002. Hafnium isotopes in basalts from the southern Mid-Atlantic Ridge from 40°S to 55°S: discovery and Shona plume-ridge interactions and the role of recycled sediments. Geochemistry Geophysics Geosystems 3. doi:10.1029/2002GC000324 article 8502.
Arndt, N.T., Goldstein, S.L., 1989. An open boundary between lower continental crust and mantle: its role in crust formation and recycling. Tectonophysics 161, 201–212.
Arndt, N.T., Christensen, U., 1992. The role of lithospheric mantle in continental flood volcanism: thermal and geochemical constraints. Journal of Geophysical Research 97, 10967–10981.
Batiza, R., Fox, P.J., Vogt, P.R., Cande, S.C., Grindlay, N.R., Melson, W.G., O'Hearn, T., 1989. Morphology, abundance and chemistry of near-ridge seamounts in the vicinity of the Mid-Atlantic Ridge ~26°S. Journal of Geology 97, 209–220.
Batiza, R., Nelson, W.G., O'Hearn, T., 1988. Simple magma supply geometry inferred beneath a segment of the Mid-Atlantic Ridge. Nature 335, 428–431.
Blackman, D.K., Forsyth, D.W., 1991. Isostatic compensation of tectonic features of the Mid-Atlantic Ridge: 25°27′30′S. Journal of Geophysical Research 96, 11741–11758.
Borisova, A., Belyatsky, B.V., Portnyagin, M.V., Sushchevskaya, N.M., 2001. Petrogenesis of olivine-phyric basalts from the Aphanasey–Nitikin Rise: evidence for contamination by cratonic lower continental crust. Journal of Petrology 42, 277–319.
Carbotte, S.M., Welch, Macdonald, K.C., 1991. Spreading rate, rift valley propagation, and fracture zone offset history during the past 5 my on the Mid-Atlantic Ridge: 25°–27°30′S and 31°–34°30′S. Marine Geophysical Researches 13, 51–80.
Castillo, P.R., 1988. The Dupal anomaly as a trace of the upwelling lower mantle. Nature 336, 667–670.
Castillo, P.R., Batiza, R., 1989. Strontium, neodymium and lead isotope constraints on near-ridge seamount production beneath the South Atlantic. Nature 342, 262–265.
Chaffey, D.J., Cliff, R.A., Wilson, B.M., 1989. Characterisation of the St Helena magma source. Journal of the Geological Society London Special Publication 42, 257–276.
Chauvel, C., Hémond, C., 2000. Melting of a complete section of oceanic crust: trace element and Pb isotopic evidence from Iceland. Geochemistry Geophysics Geosystems 1 article 1999GC000002.
Chesley, J.T., Ruiz, J., 1998. Crust–mantle interaction in large igneous provinces: implications from the Re–Os isotope systematics of the Columbia River flood basalts. Earth and Planetary Science Letters 154, 1–11.
Class, C., le Roex, A.P., 2006. Continental material in the shallow oceanic mantle: how does it get there? Geology 34, 129–132.
Coogan, L.A., MacLeod, C.J., Dick, H.L.B., Edwards, S.J., Kvassnes, A., Natland, J.H., Robinson, P.T., Thompson, G., O'Hara, M.J., 2001. Whole-rock geochemistry of gabbros from the Southwest Indian Ridge: constraints on geochemical fractionations between the upper and lower oceanic crust and magma chamber processes at (very) slow-spreading ridges. Chemical Geology 178, 1–22.
Danyushevsky, L.V., Perfit, M., Eggins, S.M., Falloon, T.J., 2001. Crustal origin for coupled 'ultra-depleted' and 'plagioclase' signatures in MORB olivine-hosted melt inclusions: evidence from the Siqueiros Transform Fault, East Pacific Rise. Contributions to Mineralogy and Petrology 144, 619–637.
Deng, J., Su, S., Niu, Y.L., Liu, C., Zhao, G., Zhao, X., Zhou, S., Wu, Z., 2007. A possible model for the lithospheric thinning of North China Craton: evidence from the Yanshanian (Jura-Cretaceous) magmatism and tectonic deformation. Lithos 96, 22–35.
Douglass, J., Schilling, J.-G., Fontignie, D., 1999. Plume–ridge interactions of the discovery and Shona mantle plumes with the southern Mid-Atlantic Ridge (40°–55°S). Journal of Geophysical Research 104, 2941–2962.
Douglass, J., Schilling, J.-G., 2000. Systematics of three-component, pseudo-binary mixing lines in 2D isotope ratio space: representations and implications for mantle plume–ridge interaction. Chemical Geology 163, 1–23.
Dunai, T.J., Touret, J.L.R., 1993. A noble gas study of a granulite sample from the Nilgiri Hills, southern India: implications for granulite formation. Earth and Planetary Science Letters 119, 271–281.
Dupré, B., Allègre, C.J., 1983. Pb–Sr isotope variation in Indian Ocean basalts and mixing phenomena. Nature 303, 142–146.
Elkins-Tanton, L.T., 2005. Continental magmatism caused by lithospheric delamination. Geological Society of America Special Publication 388, 449–461.
Elkins-Tanton, L.T., Hager, B.H., 2000. Melt intrusion as a trigger for lithospheric foundering and the eruption of the Siberian flood basalts. Geophysical Research Letters 27, 3937–3940.
Escrig, S., Schiano, P., Schilling, J.-G., Allègre, C., 2005. Rhenium–osmium isotope systematics in MORB from the Southern Mid-Atlantic Ridge (40–50°S). Earth and Planetary Science Letters 235, 528–548.
Fontignie, D., Schilling, J.-G., 1996. Mantle heterogeneities beneath the South Atlantic: a Nd–Sr–Pb isotope study along the Mid-Atlantic Ridge (3°S–46°S). Earth and Planetary Science Letters 142, 209–221.
Frey, F.A., Weis, D., Borisova, A., Xu, G., 2002. Involvement of continental crust in the formation of the Cretaceous Kerguelen Plateau: new perspectives from ODP Leg 120 sites. Journal of Petrology 43, 1207–1239.
Galer, S.J.G., 1999. Optimal double and triple spiking for high precision lead isotopic measurement. Chemical Geology 157, 255–274.
Gallagher, K., Hawkesworth, C.J., 1992. Dehydration melting and the generation of continental flood basalts. Nature 358, 57–59.
Gallagher, K., Hawkesworth, C.J., Mantovani, M.S.M., 1994. The denudation history of the onshore continental margin of SE Brazil inferred from apatite fission track data. Journal of Geophysical Research 99, 18117–18145.
Gasperini, D., Blichert-Toft, J., Bosch, D., Del Moro, A., Macera, P., Télouk, P., Albarède, F., 2000. Evidence from Sardinian basalt geochemistry for recycling of plume heads into the Earth's mantle. Nature 408, 701–704.
Gibson, S.A., Thompson, R.N., Day, J.A., Humphris, S.E., Dickin, A.P., 2005. Melt generation processes associated with the Tristan mantle plume: constraints on the origin of EM-1. Earth and Planetary Science Letters 237, 744–767.
Graham, D.W., Castillo, P.R., Lupton, J.E., Batiza, R., 1996. Correlated He and Sr isotope ratios in South Atlantic near-ridge seamounts and implications for mantle dynamics. Earth and Planetary Science Letters 144, 491–503.
Graham, D.W., Jenkins, W.J., Schilling, J.-G., Thompson, G., Kurz, M.D., Humphris, S.E., 1992. Helium isotope geochemistry of mid-ocean ridge basalts from the South Atlantic. Earth and Planetary Science Letters 110, 133–147.
Grindlay, N.R., Fox, P.J., Vogt, P.R., 1992. Morphology and tectonics of the Mid-Atlantic Ridge (26°–27°30′S) from Sea Beam and magnetic data. Journal of Geophysical Research 97, 6983–7010.
Gurenko, A.A., Sobolev, A.V., 2006. Crust-primitive magma interaction beneath neovolcanic rift zone of Iceland recorded in gabbro xenoliths from Midfell, SW Iceland. Contributions to Mineralogy and Petrology 151, 495–520.
Hales, T.C., Abt, D.K., Humphreys, E.D., Roering, J.J., 2005. A lithospheric instability origin for Columbia River flood basalts and Wallowa Mountains uplift in northeast Oregon. Nature 438, 842–845.
Halliday, A., Lee, D., Tommasini, S., Davies, G., Paslick, C., Fitton, J., James, D., 1995. Incompatible trace elements in OIB and MORB and source enrichment in the sub-oceanic mantle. Earth and Planetary Science Letters 133, 379–395.
Hanan, B.B., Kingsley, R.H., Schilling, J.-G., 1986. Pb isotope evidence in the South Atlantic for migrating ridge hotspot interactions. Nature 322, 137–144.
Hanan, B.B., Blichert-Toft, J., Pyle, D.G., Christie, D.M., 2004. Contrasting origins of the upper mantle revealed by hafnium and lead isotopes from the Southeast Indian Ridge. Nature 432, 91–94.
Hannigan, R.E., Basu, A.R., Teichmann, F., 2001. Mantle reservoir geochemistry from statistical analysis of ICP-MS trace element data of equatorial mid-Atlantic MORB glasses. Chemical Geology 175, 397–428.
Hart, S.R., 1984. A large scale isotopic anomaly in the Southern Hemisphere mantle. Nature 309, 753–757.
Hart, S.R., Blusztain, J., Dick, H.J.P., Meyer, P.S., Muehlenbachs, K., 1999. The fingerprint of seawater circulation in a 500-meter section of ocean crust gabbro. Geochimica et Cosmochimica Acta 63, 4059–4080.
Hawkesworth, C.J., Mantovani, M.S.M., Taylor, P.N., Palacz, Z., 1986. Evidence from the Parana of south Brazil for a continental contribution to Dupal basalts. Nature 322, 356–359.
Hawkesworth, C.J., Mantovani, M.S.M., Peate, D.W., 1988. Lithosphere remobilisation during Parana CFB magmatism. Journal of Petrology 205–223 (special volume).

Hémond, C., Arndt, N.T., Lichtenstein, U., Hofmann, A.W., Oskarsson, N., Steinthorsson, S., 1993. The heterogeneous Iceland plume: Nd–Sr–O isotopes and trace element constraints. Journal of Geophysical Research 98, 15833–15850.
Hill, R.I., Campbell, I.H., Davies, G.F., Griffiths, R.W., 1992. Mantle plumes and continental tectonics. Science 256, 186–193.
Hofmann, A.W., White, W.M., 1983. Ba, Rb and Cs in the Earth's mantle. Zeitschrift fur Naturforschung 38a, 256–266.
Hofmann, A.W., Jochum, K.P., Seufert, M., White, W.M., 1986. Nb and Pb in oceanic basalts: new constraints on mantle evolution. Earth and Planetary Science Letters 79, 33–45.
Hofmann, A.W., Jochum, K.P., 1996. Source characteristics derived from very incompatible trace elements in Mauna Loa and Mauna Kea basalts, Hawaii Scientific Drilling Project. Journal of Geophysical Research 101, 11831–11839.
Humphris, S.E., Thompson, G., 1982. A geochemical study of rocks from the Walvis Ridge, South Atlantic. Chemical Geology 36, 253–274.
Humphris, S.E., Thompson, G., Schilling, J.-G., Kingsley, R.H., 1985. Petrological and geochemical variations along the Mid Atlantic Ridge between 46°S and 32°S: influence of the Tristan da Cunha mantle plume. Geochimica et Cosmochimica Acta 49, 1445–1464.
Janney, P.E., le Roex, A.P., Carlson, R.W., 2005. Hafmium isotope and trace element constraints on the nature of mantle heterogeneity beneath the Central Southwest Indian Ridge (13°E to 47°E). Journal of Petrology 46, 2427–2464.
Kamenetsky, V.S., Maas, R., Norman, M.D., Cartwright, I., Peyve, A.A., 2001. Remnants of Gondwanan continental lithosphere in oceanic upper mantle: evidence from the South Atlantic Ridge. Geology 29, 243–246.
Kay, R.W., Kay, S.M., 1993. Delamination and delamination magmatism. Tectonophysics 219, 177–189.
Kramers, J.D., Tolstikhin, I.N., 1997. Two terrestial Pb isotope paradoxes, forward transport modelling, core formation and the history of the continental crust. Chemical Geology 139, 75–110.
le Roex, A.P., Cliff, R.A., Adair, B.J.I., 1990. Tristan da Cunha, South Atlantic: geochemistry and petrogenesis of a basanite–phonolite lava series. Journal of Petrology 31, 779–812.
le Roux, P.J., le Roex, A.P., Schilling, J.-G., Shimizu, N., Perkins, W.W., Pearce, N.J.G., 2002. Mantle heterogeneity beneath the southern Mid-Atlantic Ridge: trace element evidence for contamination of ambient asthenospheric mantle. Earth and Planetary Science Letters 203, 479–498.
Lundstrom, C.C., Gill, J., Williams, Q., Hanan, B.B., 1998. Investigating solid mantle upwelling beneath mid-ocean ridges using U-series disequilibria. II. A local study at 33°S Mid-Atlantic Ridge. Earth and Planetary Science Letters 157, 167–181.
Lustrino, M., Dallai, L., 2003. On the origin of EM-1 end-member. Neues Jahrbuch fur Mineralogie Abhandlungen 179, 85–100.
Lustrino, M., 2005. How the delamination and detachment of lower crust can influence basaltic magmatism. Earth Science Reviews 72, 21–38.
Mahoney, J.J., le Roex, A.P., Peng, Z., Fisher, R.L., Natland, J.H., 1992. Southwestern limits of Indian Ocean Ridge mantle and the origin of low $^{206}Pb/^{204}Pb$ mid-ocean ridge basalt: isotope systematics of the Central Southwest Indian Ridge (17–50°E). Journal of Geophysical Research 97, 19771–19790.
Mahoney, J.J., White, W.M., Upton, G.G.J., Neal, C.R., Scrutton, R.A., 1996. Beyond EM-1: lavas from Afanasy–Nitikin Rise and the Crozet Archipelago, Indian Ocean. Geology 24, 615–618.
McDonough, W.F., 1990. Constraints on the composition of the continental lithospheric mantle. Earth and Planetary Science Letters 101, 1–18.
Menzies, M.A., 1992. The lower lithosphere as a major source for continental flood basalts: a re-appraisal. Geological Society of London Special Publication 68, 31–39.
Meyzen, C.M., Ludden, J.N., Humler, E., Luais, B., Toplis, M.J., Mével, C., Storey, M., 2005. New insights into the origin and distribution of the DUPAL isotope anomaly in the Indian Ocean mantle from MORB of the Southwest Indian Ridge. Geochemistry Geophysics Geosystems 6. doi:10.1029/2005GC000979 article Q11K11.
Michael, P.J., Forsyth, D.W., Blackman, D.K., Fox, P.J., Hanan, B.B., Harding, A.J., Macdonald, K.C., Neumann, G.A., Orcutt, J.A., Tolstoy, M., Weiland, C.M., 1994. Mantle control of a dynamically evolving spreading center: Mid-Atlantic Ridge 31–34°S. Earth and Planetary Science Letters 121, 451–468.
Milner, S.C., le Roex, A.P., 1996. Isotope characteristics of the Okenyenya igneous complex, northwestern Namibia: constraints on the composition of the early Tristan plume and the origin of the EM1 mantle component. Earth and Planetary Science Letters 141, 277–291.
Moreira, M., Kurz, M.D., 2001. Subducted oceanic lithosphere and the origin of the 'high μ' basalt helium isotopic signature. Earth and Planetary Science Letters 189, 49–57.
Niu, Y., Batiza, R., 1994. Magmatic processes at a slow spreading ridge segment: 26°S Mid-Atlantic Ridge. Journal of Geophysical Research 99, 19719–19740.
Niu, Y., Batiza, R., 1997. Trace element evidence from seamounts for recycled oceanic crust in the eastern Pacific mantle. Earth and Planetary Science Letters 148, 471–483.
Niu, Y., Collerson, K.D., Batiza, R., Wendt, J.I., Regelous, M., 1999. Origin of enriched-type mid-ocean ridge basalt at ridges far from mantle plumes: the East Pacific Rise at 11°20′N. Journal of Geophysical Research 104, 7067–7087.
Niu, Y., O Hara, M.J., 2006. MORB mantle hosts the missing Eu in the continental crust. Geochimica et Cosmochimica Acta 70, A447 (abstract).
Niu, Y., Bideau, D., Hékinian, R., Batiza, R., 2001. Mantle compositional control on the extent of mantle melting, crust production, gravity anomaly and ridge morphology: a case study at the Mid Atlantic Ridge 33–35°N. Earth and Planetary Science Letters 186, 383–399.
Niu, Y., 2005. Generation and evolution of basaltic magmas: some basic concepts and a new view on the origin of Mesozoic–Cenozoic basaltic volcanism in eastern China. Geological Journal of China Universities 11, 9–46.
Niu, Y., Regelous, M., Wendt, J.I., Batiza, R., O'Hara, M.J., 2002. Geochemistry of near-EPR seamounts: importance of source vs. process and the origin of enriched mantle component. Earth and Planetary Science Letters 199, 329–348.
Peate, D.W., Hawkesworth, C.J., Mantovani, M.S.M., Rogers, N.W., Turner, S.P., 1999. Petrogenesis and stratigraphy of the high-Ti/Y Urubici magma type in the Parana flood basalt province and implications for the nature of 'Dupal'-type mantle in the South Atlantic region. Journal of Petrology 40, 451–473.
Peng, Z.X., Mahoney, J.J., Hooper, P., Harris, C., Beane, J., 1994. A role for lower continental crust in flood basalt genesis? Isotopic and incompatible element study of the lower six formations of the western Deccan Traps. Geochimica et Cosmochimica Acta 58, 267–288.
Pilot, J., Werner, C.D., Haubrich, F., Baumann, N., 1998. Palaeozoic and Proterozoic zircons from the Mid-Atlantic Ridge. Nature 393, 676–679.
Plank, T., Langmuir, C.H., 1998. The chemical composition of subducting sediment and its consequences for the crust and mantle. Chemical Geology 145, 325–394.
Regelous, M., Niu, Y., Wendt, J.I., Batiza, R., Grieg, A., Collerson, K.D., 1999. Variations in the geochemistry of magmatism on the East Pacific Rise at 10°30′N since 800 ka. Earth and Planetary Science Letters 168, 45–63.
Regelous, M., Hofmann, A.W., Abouchami, W., Galer, S.J.G., 2002. Geochemistry of lavas from the Emperor Seamounts, and the geochemical evolution of Hawaiian magmatism from 85 to 43 Ma. Journal of Petrology 44, 113–140.
Renne, P.R., Ernesto, M., Pacca, R.S., Glen, J.M., Prevot, M., Perrin, M., 1992. The age of Parana flood volcanism, rifting of Gondwanaland, and the Jurassic–Cretaceous boundary. Science 258, 975–979.
Richardson, S.H., Erlank, A.J., Duncan, A.R., Reid, D.L., 1982. Correlated Nd, Sr and Pb isotope variation in Walvis Ridge basalts and implications for the evolution of their mantle source. Earth and Planetary Science Letters 59, 327–342.
Rudnick, R.L., Fountain, D.M., 1995. Nature and composition of the continental crust: a lower crustal perspective. Reviews in Geophysics 33, 267–309.
Rudnick, R.L., 1995. Making continental crust. Nature 378, 571–578.
Rudnick, R.L., Gao, S., 2003. Composition of the continental crust. In: Rudnick, R.L. (Ed.), The Crust. Treatise in Geochemistry, vol. 3, pp. 1–64.
Saal, A.E., Kurz, M.D., Hart, S.R., Blusztajn, J.S., Blichert-Toft, J., Liang, Y., Geist, D.J., 2007. The role of lithospheric gabbros on the composition of Galapagos lavas. Earth and Planetary Science Letters 257, 391–406.
Schilling, J.-G., Thompson, G., Kingsley, R.H., Humphris, S.E., 1985. Hotspot-migrating ridge interactions along the South Atlantic: geochemical evidence. Nature 313, 187–191.
Siebel, W., Becchio, R., Volker, F., Hansen, M.A.F., Viramonte, J., Trumbull, R.B., Haase, G., Zimmer, M., 2000. Trinidade and Martin Vaz Islands, South Atlantic: isotopic (Sr, Nd, Pb) and trace element constraints on plume related magmatism. Journal of South American Earth Science 13, 79–103.
Sobolev, A.V., Hofmann, A.W., Nikogosian, I.K., 2000. Recycled oceanic crust observed in 'ghost plagioclase' within the source of Mauna Loa lavas. Nature 404, 986–990.
Stracke, A., Bizimis, M., Salters, V.J.M., 2003. Recycling oceanic crust: quantitative constraints. Geochemistry Geophysics Geosystems 4. doi:10.1029/2001GC000223 article 8003.
Tatsumi, Y., 2000. Continental crust formation by crustal delamination in subduction zones and complementary accumulation of the enriched mantle 1 component in the mantle. Geochemistry Geophysics Geosystems 1 2000GC000094.
Taylor, S.R., McLennan, S.M., 1985. The Continental Crust: Its Composition and Evolution. Blackwell, Oxford. 312 pp.
Turner, S., Regelous, M., Kelley, S., Hawkesworth, C.J., Mantovani, M.S.M., 1994. Magmatism and continental breakup in the South Atlantic: high precision $^{40}Ar$–$^{39}Ar$ geochronology. Earth and Planetary Science Letters 121, 333–348.
Weaver, B.L., Wood, D.A., Tarney, J., Joron, J.L., 1987. Geochemistry of ocean island basalts from the South Atlantic: Ascension, Bouvet, St. Helena, Gough and Tristan da Cunha. In: Fitton, J.G., Upton, B.G.J. (Eds.), Alkaline Igneous Rocks. Geological Society of London Special Publication, vol. 30, pp. 253–267.
Wendt, J.I., Regelous, M., Niu, Y., Hékinian, R., Collerson, K.D., 1999. Geochemistry of lavas from the Garrett Transform Fault: insights into mantle heterogeneity beneath the eastern Pacific. Earth and Planetary Science Letters 173, 271–284.
White, W.M., Hofmann, A.W., Puchelt, H., 1987. Isotope geochemistry of Pacific mid-ocean ridge basalt. Journal of Geophysical Research 92, 4881–4893.
Willbold, M., Stracke, A., 2006. Trace element composition of mantle end-members: implications for recycling of oceanic and upper and lower continental crust. Geochemistry Geophysics Geosystems 7. doi:10.1029/2005GC001005 article Q04004.
Yang, H.-J., Frey, F.A., Weis, D., Giret, A., Pyle, D., Michon, G., 1998. Petrogenesis of the flood basalts forming the northern Kerguelen Archipelago: implications for the Kerguelen plume. Journal of Petrology 39, 711–748.
Zartman, R.E., Haines, S.M., 1988. The plumbotectonic model for Pb isotopic systematics among major terrestrial reservoirs — a case for bi-directional transport. Geochimica et Cosmochimica Acta 52, 1327–1339.